

الجمهورية الجزائرية الديمقراطية الشعبية
République algérienne démocratique et populaire
وزارة التعليم العالي والبحث العلمي
Ministère de l'enseignement supérieur et de la recherche scientifique
جامعة عين تموشنت بلحاج بوشعيب
Université –Ain Temouchent- Belhadj Bouchaib
Faculté des Sciences et de Technologie
Département de Génie Mécanique



End of Study Project
For the Master's Degree
Domain : Science and Technology
Branch : Mechanical Engineering
Speciality: Energy
Theme

Digital improvement of the performance of a solar air collector with wavy-shaped baffles

Presented by :

- 1) Melle. BOUCHIKHI Rania
- 2) M. AID Abdelbasset

In front of the jury composed of:

Pr.BENSAAD Bourassia	Prof	UAT.B.B (Ain Temouchent)	President
Dr.DORBANE Abdelhakim	MCA	UAT.B.B (Ain Temouchent)	Examiner
Pr.BENZENINE Hamidou	Prof	UAT.B.B (Ain Temouchent)	Encadrant
Dr. BOUCETTA Abdelkader	Researcher	Université Sorbonne Paris Nord)	Co-Encadrant

University Year 2023/2024

Dedication

I would like to dedicate this work firstly to my mom DARDEK Samira who was there for me as well as my family, everyone who helped me, my classmates of energetic and my friends who supported me throughout this journey.

BOUCHIKHI Rania

I dedicate this work firstly to my parents and my family, secondly to everyone who taught me, and thirdly to my friends

AID Abdelbasset

Acknowledgments

Firstly thanks to Allah, who helped and guided us.

We would like to express our gratitude to our supervisors Prof. Hamidou BENZENINE from the University of Ain Temouchent and Dr. Abdelkader BOUCETTA from Sorbonne Paris University who suggested this project and generously gave us enlightenment throughout this work.

To Professor Bourassia BENZAAD, professor at the University of Ain Temouchent, who gave us the honor to accept the presidency of the jury in testimony of our respect, sincere thanks.

To doctor Abdelhakim DORBANE, doctor at the University of Ain Temouchent, who accepted to judge this work and be part of the jury of our work in the testimony of our respect, sincere thanks.

Our gratitude is due to the head and staff of both the mechanical department and energy laboratory for their help and support in our research.

Finally, thanks to anyone who helped in one way or another in bringing out this work.

Abstract

In this work, we investigated numerically the thermal and dynamic characteristics of a convective flow in a flat-solar collector with single-pass air. The continuity, momentum, and energy equations govern the flow inside the restricted area between the insulation and the glass. The geometric configuration and the governing equations are solved by the ANSYS FLUENT code, which is based on the finite volume method. The turbulence model ($k-\varepsilon$) is used to model the turbulence. This study shows the influence on the performance of the collector using wavy-shaped baffles, the impact of temperature and flux heat on its efficiency for different heights and baffles positions.

Keywords: flat-solar collector, ANSYS FLUENT, thermal efficiency

Résumé

Dans ce travail, nous avons étudié numériquement les caractéristiques thermiques et dynamiques d'un flux convectif dans un collecteur solaire plan d'air à un seul passage. Les équations de continuité, de mouvement et d'énergie contrôlent le flux de chaleur à l'intérieur de la zone entre l'isolant et le verre. La configuration géométrique et les équations gouvernante sont résolues par le code ANSYS FLUENT, qui est basé sur la méthode des volumes finis. Le modèle de turbulence ($k-\varepsilon$) est utilisé pour modéliser la Turbulence. Cette étude montre l'influence de l'adjonction des ailettes de forme ondulée sur les performances de ce collecteur, l'impact de la température et le flux de chaleur sur son efficacité a été également étudié pour différentes hauteur et positionnement de ces ailettes.

Mots clés: collecteur solaire plan, ANSYS FLUENT, efficacité thermique.

المخلص

في هذا العمل، قمنا بدراسة عددية للسلوك الديناميكي والحراري لتدفق الحمل الحراري في لاقط شمسي هوائي مستوي بممر فردي. فالاستمرارية والحركة ومعادلات الطاقة تحكم التدفق داخل المنطقة المقيدة بين العازل والزجاج. يتم حل التشكيل الهندسي ومعادلات التحكم بواسطة رمز انسيس فليانت، الذي يقوم على طريقة الحجم المحدود. ويُستخدم نموذج الاضطراب (k-ε) لتصوير التوترات. تظهر هذه الدراسة تأثير إضافة زعانف على أداء هذا اللاقط الشمسي، وتأثير درجة الحرارة والتدفق الحراري على فعاليته أيضاً، وقد تم دراسة على ارتفاع وتموضع مختلف لهذه زعانف.

الكلمات مفتاحية: اللاقط الشمسي، انسيس فليانت، كفاءة حرارية.

Nomenclature and abbreviations

A	Section area	m^2
C_p	Specific heat	$J\ kg^{-1}\ ^\circ K^{-1}$
C_{ε1}, C_{ε2}, C_{ε3}, C_μ	Empirical constants for the <i>k-ε</i> turbulence model	
h	Heat transfert coefficient	$W\ m^{-2}\ ^\circ k^{-1}$
k	Turbulent kinetic energy	$J\ kg^{-1} = m^2\ s^{-2}$
Lc	Characteristic dimension	m
S_φ	Source term	
T	Temperature	$^\circ C$ or $^\circ k$
U	Flow mean velocity	$m\ s^{-1}$
U_{wind}	Wind velocity	$m\ s^{-1}$
V	Velocity	$m\ h^{-1}$
R	Radius	cm
L	Length	cm
W	width	cm
H	Height	m

• Greek symbols

λ	Thermal conductivity	$W\ m^{-1}\ ^\circ k^{-1}$
ρ	Density	$Kg\ m^{-3}$
ν	kinematic viscosity	$m^2\ s^{-1}$
μ	Dynamic viscosity	$Kg\ m^{-1}\ s^{-1}$
μ_t	Turbulent or eddy viscosity	$Kg\ m^{-1}\ s^{-1}$
φ	Viscous dissipation function	
Γ	Diffusion coefficient	
ε	Turbulence kinetic energy dissipation rate	$m^2\ s^{-3}$
τ_w	Wall shear stress	$Pa = kg\ m^{-1}\ s^{-2}$
σ_ε, σ_k	Empirical constants for the for the <i>k-ε</i> turbulence model	

- **Dimensionless terms**

Re	Reynolds number
Nu	Nusselt number
Pr	Prandtl number
Cf	Friction coefficient

- **Abbreviations**

MFV	Method Finite Volume
CFD	Computational fluid dynamics

Summary

<i>Dedication</i>	I
<i>Acknowledgments</i>	II
<i>Abstract</i>	III
<i>Résumé</i>	III
<i>الملخص</i>	IV
<i>Summary</i>	V
<i>List of Figures</i>	VIII
<i>List of tables</i>	X
<i>Nomenclature and abbreviations</i>	XII
General Introduction.....	2

Chapter I: General information on solar collector

I.1 Introduction	4
I.2 History of Thermal Solar Collector	4
I.3 Definition of thermal solar collector.....	6
I.4 Types of heat transfer.....	7
I.4.1 Convection.....	7
I.4.2 Conduction	7
I.4.3 Radiation.....	7
I.5 The solar collector components.....	9
I.5.1 Transparent cover (glass).....	9
I.5.2 Absorber	9
I.5.3 Thermal Insulation	9
I.5.4 Sensor case	10

I.6 Solar Collector Principles of Operation.....	10
I.7 solar collector types	11
I.7.1 Tank-type collector	11
I.7.2 Pool Collector.....	11
I.7.3 flat-plate collector	11
I.7.3.1 Single-pass flat-plate collector.....	11
I.7.3.2 Double-pass flat-plate collector	12
I.7.4 Evacuated tube collector.....	14
I.7.5 Concentrating Collector.....	15
I.7.5.1 Line Focus Collectors.....	15
I.7.5.2 Point Focus Collectors.....	16
I.8 Advantages and disadvantages of solar power plant	17
I.8.1 Advantages of Solar Power Plant.....	17
I.8.2 Disadvantages of Solar Power Plant	17
I.9 Application of solar collector	18
I.10 Conclusion.....	18
References	19

Chapter II: Bibliographic Research

II.1 Introduction	22
II.2 Research on single-pass solar collector.....	22
II.3 Research on double-pass solar collectors.....	27
II.4 Conclusion.....	36
References	37

Chapter III: Mathematical formulation and numerical modeling

III.1 Introduction.....	40
III.2 Main methods of discretion	40
III.2.1 Finite deference	40
III.2.2 Finite elements.....	40
III.2.3 Finite volume method.....	40
III.3 Governing Equations.....	42
III.4 Closure Templates.....	44
III.4.1 (k- ε) Model.....	45
III.5 ANSYS FLUENT definition	47
III.6 Problem Geometry	47
III.7 Mathematical formulation.....	51
III.7.1 Simplified Assumptions	51
III.7.2 Limit Conditions.....	51
III.7.3 Characteristic Settings.....	52
III.8 Conclusion	53
References	54

Chapter IV: Interpretation of the results and discussion

IV.1 Introduction.....	57
IV.2 Validation.....	57
IV.3 Results and interpretation.....	58
IV.3.1 Dynamic aspect	58
IV.3.2 Thermal aspect.....	62
IV.4 Conclusion	68
References	69
General conclusion.....	71

List of Figures

Figure I. 1: Illustration of the three main physical mechanisms of heat transfer: convection, conduction, and radiation	8
Figure I.2: Water Flat Collector Scheme	9
Figure I.3: Typical construction of a flat-plate solar thermal collector.....	10
Figure I.4: simple-pass solar collector.....	12
Figure I.5: double-pass flat-plate solar collector.	13
Figure I.6: Classification of flat-plate solar collectors	13
Figure I.7: Classification of an evacuated solar collector.....	14
Figure I.8: A diagram of a line focus solar collector.....	16
Figure I.9: A point-focus solar collector.	16
Figure II.1: Solar collector components	22
Figure II. 2: Disposal of obstacles D.....	23
Figure II.3: Disposal of obstacles OCL.....	23
Figure II.4: collector with obstacles TL.	23
Figure II.5: Dandail in air channel duct.	24
Figure II.6: Collector with finned system on the back wooden plate.	24
Figure II.7: Different positions of cylindrical roughness.....	25
Figure II.8: The schematic of an experimental device.....	26
Figure II.9: a description of the baffle schematic.....	26
Figure II.10: Absorber with baffles in semi-cylindrical shape.	27
Figure II.11: The schematic of a double-pass thermal solar collector with porous media in the second channel.....	28
Figure II.12: Schematic diagram of the solar air heater	29
Figure II.13: flat plate (1), finned (2), and v-corrugated (3) air heaters.....	30
Figure II.14: A schematic diagram of the TE solar air collector.	31
Figure II.15: Configuration 2, capsules above the absorber plate.	31
Figure II.16: Configuration 3, capsules below the absorber plate.	32
Figure II.17: Configuration 4, capsules above the back plate.	32
Figure II.18: double-pass solar collector with porous environment.....	32

Figure II.19: schematics of different used obstacles.	33
Figure II.20: the sixth studied model (N) without obstacles, (A) with rectangular obstacles, and (B) with trapezoidal obstacles.....	34
Figure II.21: Cross-sectional view of type-I SAH.	35
Figure II.22: Cross-sectional view of type-II SAH.	35
Figure II.23: Diagram of the studied solar collector.....	36
Figure III.1: Two-Dimensional Control Volume.....	41
Figure III.2: Schematic representation of a solar air collector.....	47
Figure III.3: schematic of the baffles used in the solar collector.....	48
Figure IV.1: air output Temperature of the collector (comparison with the result of AbhayLingayat et al)	58
Figure IV.2: Distribution of velocity fields attained from all studied cases.....	59
Figure IV.3: variation of the average velocity as a function of the distance of all cases.....	61
Figure IV.4: Evolution of the temperature at the collector output according to the solar radiation for all studied cases.....	62
Figure IV.5: Evolution of the temperature at the collector output according to the input velocity for all studied cases	64
Figure IV.6: Distribution of temperature fields attained from all studied cases.....	67

List of tables

Table III.1: Standard K-S model coefficients.	46
Table III.2: the baffle's dimensions	48
Table III.3: a table that shows the different baffle's positions.	50

General introduction

General Introduction

There is now a lot of research focusing on developing renewable energy sources. Numerous studies have been conducted in this area to improve energy efficiency using wind turbines, solar energy, and biomass. Some thermal applications, such as Desalination, heating homes or sanitary water, and drying agro-food products are often powered by solar energy. The solar collector is one of the systems that uses solar energy. The latter is capable of producing clean thermal energy from solar radiation. The solar collector's components are reasonably priced, and it is simple to use. Built With glass, it has a wooden structure that gives the interior a greenhouse feel. The thermal and dynamic efficiency of convective collectors has been the subject of several numerical, theoretical, and experimental studies. Some of these studies focused on enhancing the fluid properties^{1, 2}, while others increased the absorber surface area, air stream height, and air flow rate. To define the effect of the analyzed parameter, such as the heat transfer of a fluid flow and the variables influencing this system's efficiency, the form of the air and solar collector is examined.

Single-pass solar air collectors (SACs) are a simple and cost-effective technology for converting solar radiation into thermal energy for air heating applications. The performance of these collectors can be simulated mathematically, and this will help researchers improving the performance of their collectors without the need for expensive physical prototypes.

So why optimize?

The primary goal of optimization is to maximize the collector's thermal efficiency, which is the ratio of useful heat gain by the air that we can utilize for other uses such as drying or heating. That's why we created a wavy-shaped baffle using ANSYS FULENT and studied different exhibitions by comparing them to previous cases. We aimed to optimize its performance.

We started with generality on solar collector in chapter 1 followed by bibliographic research in chapter 2, chapter 3 focused on Mathematical formulation and numerical modeling finally we ended with Interpretation of the results and discussion in chapter 4 closed through a general conclusion.

Chapter I: General information on solar collector

I.1 Introduction

In this chapter, we enhance that the primary solar energy collectors is currently in use for many thermal applications such as power systems, industrial process heat, water heating, and heating and cooling of spaces outlined below. Special attention is given to the power systems that are known as solar concentrating technologies, which include solar towers, parabolic dishes, parabolic troughs, and linear Fresnel collectors. looking at the sun, not only relishing the sensation but understanding that this massive celestial body offers a solution to a crucial challenge, our perpetual demand for energy. The concept of harnessing solar power has been a longstanding dream, yet merely gazing at the sky won't unveil its full potential. involves something smaller and more intelligent, enabling us to genuinely harness that power. This marks the intriguing tale of solar energy and its covert allies, the collectors. This is where solar energy comes into play, and there are multiple options you can harness the sun's power with, ranging from large-scale installations to personal choices in your daily life.

I.2 History of thermal solar collector

The sun is a source of energy that balances human life on Earth. The use of solar thermal collectors dates back in time and they can be classified according to the different eras of technological and industrial evolution. About 212 years before Christ, Archimedes had conceived a method of producing heat using metal mirrors. In 1780 the greenhouse effect was highlighted by a glass over an absorber in an isolated box. However, it is necessary to wait until 1910 for the first solar water heaters to appear. Like many renewable energy lines, solar thermal has experienced a phase of significant growth between 1973 and 1985 in response to the oil shock. But this rapid development, with poor technologies or installers, has resulted in many counter-performance. In the late 18th century, Lavoisier built a solar oven that reached a temperature of 1800 °C. For this, it concentrates the sun's rays using a liquid lens. In 1816, Robert Stirling invented the "hot air engine" (now called the "Stirling engine"), a four-stroke engine that revolutionized the industry. During the 19th century, Augustin Mouchot developed many inventions: solar pasteurization, solar distillation, solar cooking, solar pumping, and parabolic concentrator-feeding thermal machines. He set up a 5-meter diameter reflector combined with a steam machine that drives a printing press. In 1910, Franck Shuman built an industrial-sized solar thermal power plant and it was at the end of the 20th century that various solar power plants and furnaces were launched with different prototypes, likewise, from 1984

to 1991, many parabolic cylindrical mirror plants appeared. However, Several industrial applications such as seawater desalination, energy production, drying, etc., have emerged in several countries during the last 50 years thanks to solar collectors [1].

I.3 Definition of thermal solar collector

A solar thermal collector uptake the heat energy by absorbing sunlight. The term "solar collector" commonly refers to a device for solar hot water heating, but may refer to large power-generating installations such as solar parabolic troughs and solar towers or non-water heating devices such as solar cookers, and solar air heaters [2].

Solar thermal collectors are either non-concentrating or concentrating. In non-concentrating collectors, the aperture area (i.e., the area that receives the solar radiation) is roughly the same as the absorber area (i.e., the area absorbing the radiation). A common example of such a system is a metal plate that is a dark color painting to maximize sunlight absorption. The energy is then collected by cooling the plate with a working fluid, often water or glycol running in pipes attached to the plate.

Concentrating collectors have a much larger aperture than the absorber area. The aperture is typically in the form of a mirror that is focused on the absorber, which in most cases are the pipes carrying the working fluid [3]. Due to the movement of the sun during the day, concentrating collectors often require some form of solar tracking system, and are sometimes referred to as "active" collectors for this reason.

Non-concentrating collectors are typically used in residential, industrial, and commercial buildings for space heating while concentrating collectors in concentrated solar power plants generate electricity by heating a heat-transfer fluid to drive a turbine connected to an electrical generator [4].

I.4 Types of heat transfer

We have three major types of thermal transfer:

I.4.1 Convection

Convection describes the transfer of heat by the collective motion of particles in a uniform liquid or gas. When heat transfer is due to the movement of another substance dissolved or suspended in the fluid, it may be called advection. For example, hot particles with large amounts of thermal energy "transport" heat by moving to another point in space, while the space they leave behind is filled with cooler particles, creating a net transfer in the direction of thermal energy. Particle motion thermal particles. Convection is often the dominant mechanism for heat transfer in fluids such as the Earth's atmosphere.

I.4.2 Conduction

Thermal conduction is the process by which heat spreads through diffusion. Diffusion is a micro-scale view of what is at a microscope level the propagation from close to close by shocks of the kinetic energy of agitation of atomic or electron molecules. The intensive variable "temperature" quantifies the average level of molecular agitation, while the flow of kinetic energy on a microscopic scale is equated to a flow of heat on a microscope scale [5].

The physical behavior that ensures heat transfer within a micro-scale perspective is the impact between the vibrating particles and the relatively stationary particles, which reduces the velocity of the higher velocity and increases the movements of the lower velocity particles.

I.4.3 Radiation

The heat of the Sun is transferred to the Earth without any need for a material medium and this way is known as the transfer of heat by radiation, heat is transferred by radiation through material media & non-material ones, The transfer from the heater to our bodies is by convection & radiation. The transfer of heat by radiation is the transfer from one hot object to another without any need for a medium neighborhood. The heat is transferred from all resources of light by convection and radiation, while it is transferred from the Sun by radiation only. Due to the empty intermediate space between Earth and the Sun (Quantum vacuum), the Sun's heat energy is transferred by radiation. Wearing dark clothes in winter to absorb the heat of the Sun, Wearing light colors clothes in summer to reflect the sun's rays, the Sun heat energy doesn't reach the Earth by conduction or convection, It is not transferred by conduction because the air

is a bad heat conductor and it is not transferred by convection because there is a large empty region (quantum vacuum) between the Sun & the Earth [6].

So while frequency dictates how readily light interacts with a material, the number of photons impacting a material and how they are clustered determine the overall heat transfer through energy absorption.

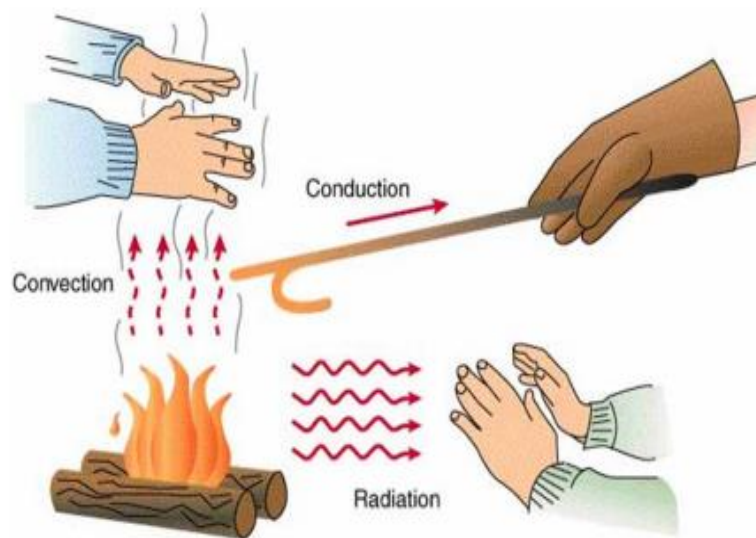


Figure I. 1: Illustration of the three main physical mechanisms of heat transfer: convection, conduction, and radiation [6].

I.5 The solar collector components

The collector is represented schematically in (Figure.I.2). It consists of a black plate (absorber), a transparent glass cover, an insulator on its rear and lateral sides, a collector safe, and an enclosure showed in figure I.2.

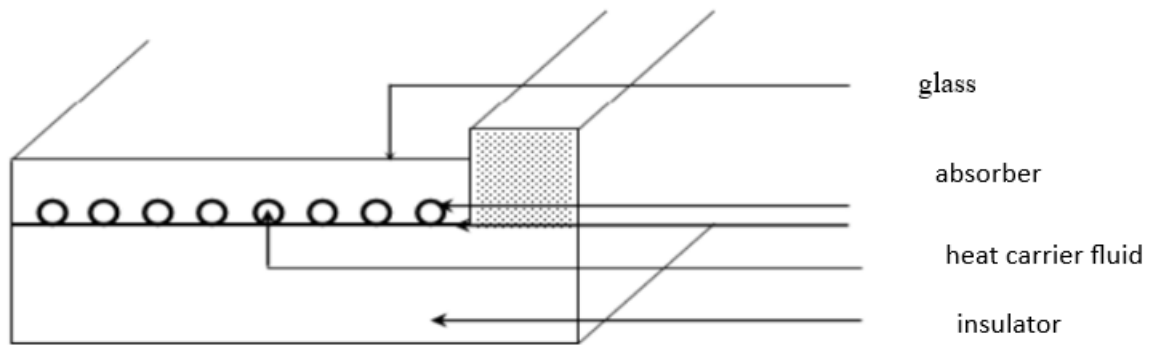


Figure I.2: Water Flat Collector Scheme [7].

I.5.1 Transparent cover (glass)

The cover has a function to protect mechanically the absorber but it also plays an important role in the thermal balance by reducing heat. Convective exchanges, which depends on the thickness of the air blade or gas located between the absorbent cover space [8].

Shocks, sudden temperature changes, and extreme temperatures must not harm the cover. It needs to be flexible, and have a low coefficient of dilation.

I.5.2 Absorber

The absorber is an essential component of the solar collector. It must absorb most of the solar radiation and transmit the heat produced to the fluid heat-bearing with a minimum loss [8].

I.5.3 Thermal insulation

The solar collector can equip one or more thermal insulating layers with thicknesses ranging from 1 to 10 cm to maximize efficiency. The most commonly used materials are wood, polystyrene, and glass wool. These insulating materials must ensure effective resistance to high temperatures, up to 200°C.

I.5.4 Collector case

The collector's safe contains various assets. It will therefore have to provide effective protection for atmospheric agents [8].

The collector cabinets are made of fine metal (galvanized steel, aluminum, or inox) with a stable covering against extreme temperatures. However, allows a good fixation with the cover and the enclosure walls, as well as permit a free manipulation. Typically, the vitrage is installed with an elastic joint that is insensitive to ultraviolet light and a mechanical profile that permits advanced assembly and disassembly procedures.

I.6 Solar Collector Principles of Operation

Solar radiation is transformed into thermal energy using a solar thermal collector, which also serves as a heat exchanger. The collector uptakes the incoming solar radiation and converts it into thermal energy. The solar energy flux (irradiance) impinges on the Earth's surface and has a fluctuating and relatively low surface density. Then the circulating fluid inside the collector receives this thermal energy. Air, water, oil, or a mixture including glycol (an antifreeze fluid) can all be used as the heat transfer fluid, particularly in forced circulation systems. At that point, the heat transfer fluid's thermal energy can be immediately employed or stored for later use. The thermal energy is transferred through convection which could be natural or forced.(figure I.3).

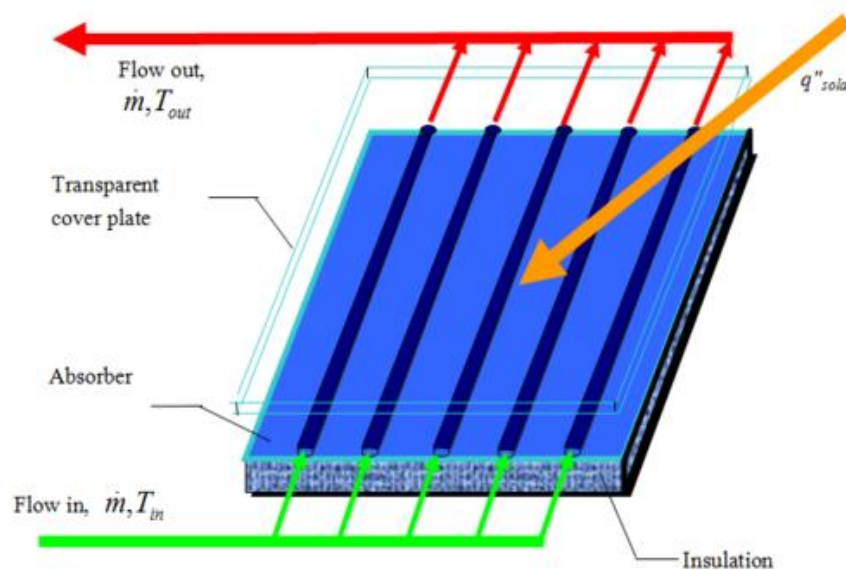


Figure I.3: Typical construction of a flat-plate solar thermal collector [9]

I.7 solar collector types

There are multiple solar collector types:

I.7.1 Tank-type collector

The solar absorber in an Integral Collector Storage unit is the hot water storage tank. The tanks are painted black or coated with a selective surface and installed in an insulating box with one side wall Glass. The sunlight entered through the glass warms the water in the black tank. The tubes are usually composed of copper, while the single tanks are often built of steel. Using such kinds of collectors, a lower temperature can be reached, rather than using flat-plate collectors.

I.7.2 Pool collector

The single largest application of active solar heating systems is the heating of swimming pools. Special collectors have been developed for heating seasonal swimming pools: they are unglazed and made of a special copolymer plastic. These collectors cannot withstand freezing conditions. The approximate maximum operating temperature of such type of solar collector is 10 – 20 °C [10] above the ambiance.

I.7.3 flat-plate collector

Flat-plate collectors are the most widely used kind of collectors in the world for domestic solar water heating and solar space heating applications [11].

I.7.3.1 Single-pass flat-plate collector

It consists of a simple glass glazing that realizes the greenhouse effect necessary to heat the absorber that is based on copper, a layer of insulation at the back of the collector, it allows a better thermal performance, ensured by polystyrene. Its particularity is that there is only one passage for the heat-bearing fluid (air).

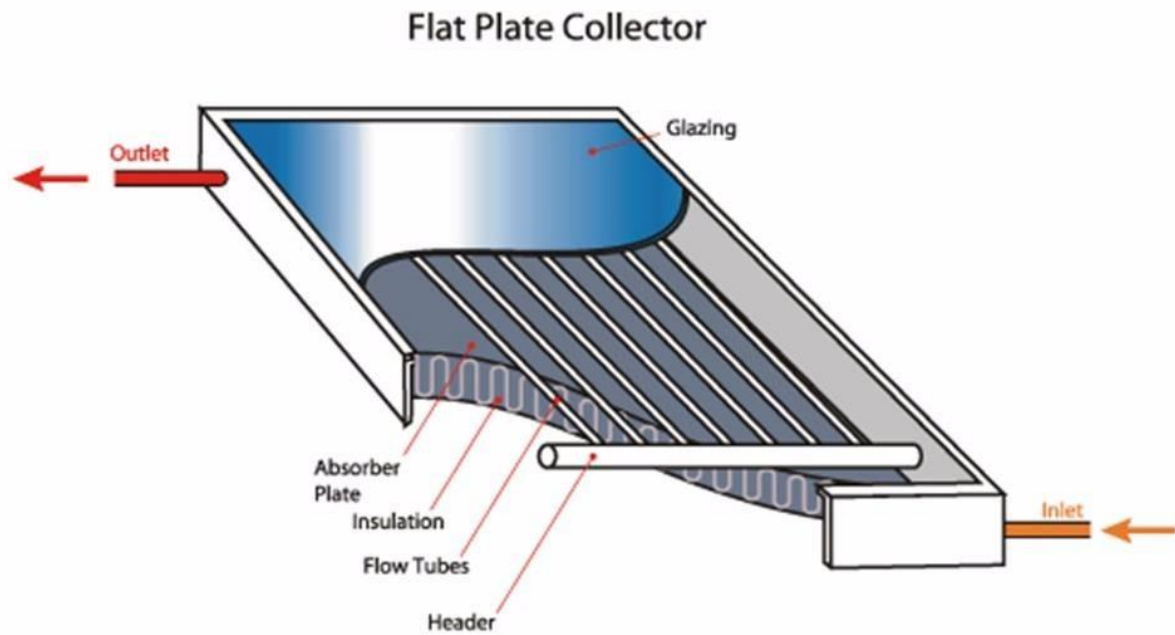


Figure I.4: simple-pass solar collector.

I.7.3.2 Double-pass flat-plate collector

Solar plane collectors with double air passes have the same principle as the simple passes, the difference relies on the level of fluid passage number. That's why the main absorbent plate element is placed in the middle of the lance. The second, pass between the cover and the plate, allows to increase the efficiency of the solar collector.

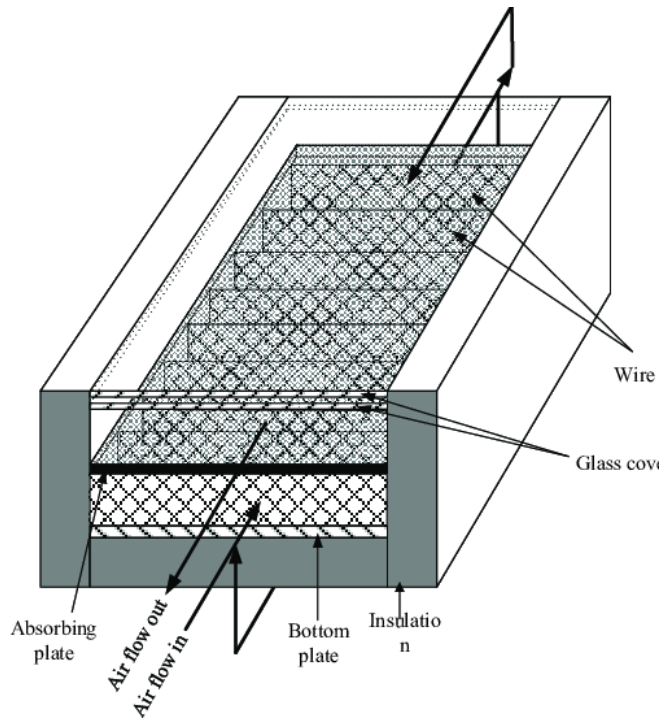


Figure I.5: double-pass flat-plate solar collector.

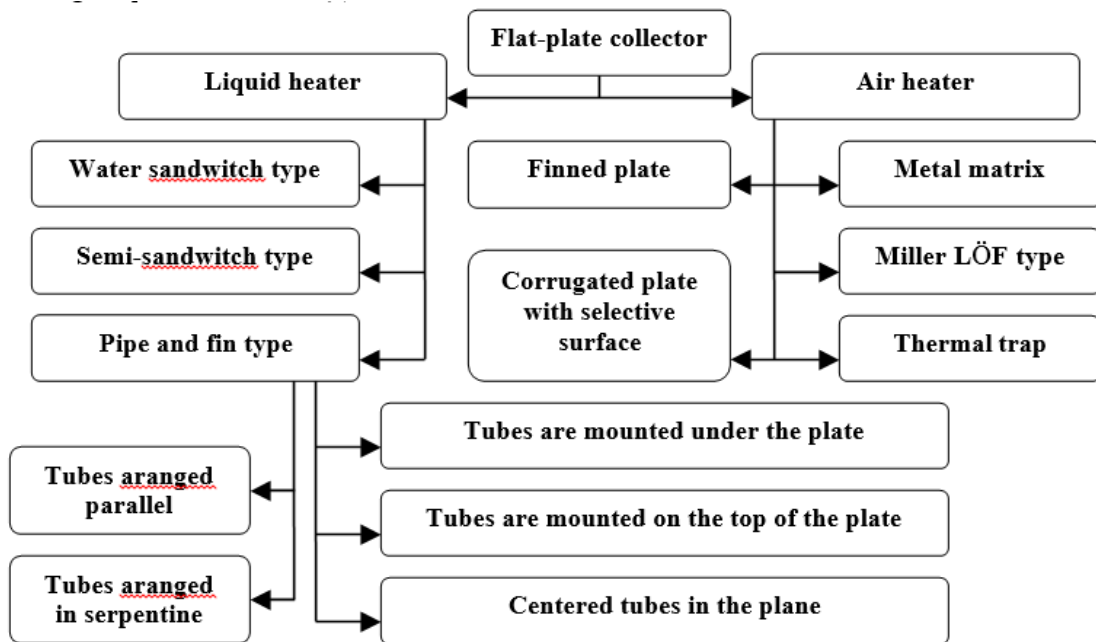


Figure I.6: Classification of flat-plate solar collectors [12].

I.7.4 Evacuated tube collector

While flat-plate collectors are all essentially have the same features and perform the same way from one brand to another. Evacuated tube collectors are constructed of a number of glass tubes, and vary widely in their construction and operation. Since the tube is a natural configuration of an evacuated collector [10], each tube is made of annealed glass and has an absorber plate within the tube. During the manufacturing process, a vacuum is created inside the glass tube in order to reduce heat losses through conduction and convection, then the balance of loss energy remain radiation phenomena [12]. The absence of air in the tube increase insulation, allowing higher temperatures to be achieved at the absorber plate. In order to improve the efficiency of evacuated tube collector, there are several types of concentrators depending on its concave radius. Fig.7 shows the classification of evacuated solar collectors. There are many possible designs of evacuated collectors, but in all of them selective coating as an absorber is used because the nonselective absorber, radiation losses would be dominated at high temperatures, and only eliminating convection would not be very effective [10].

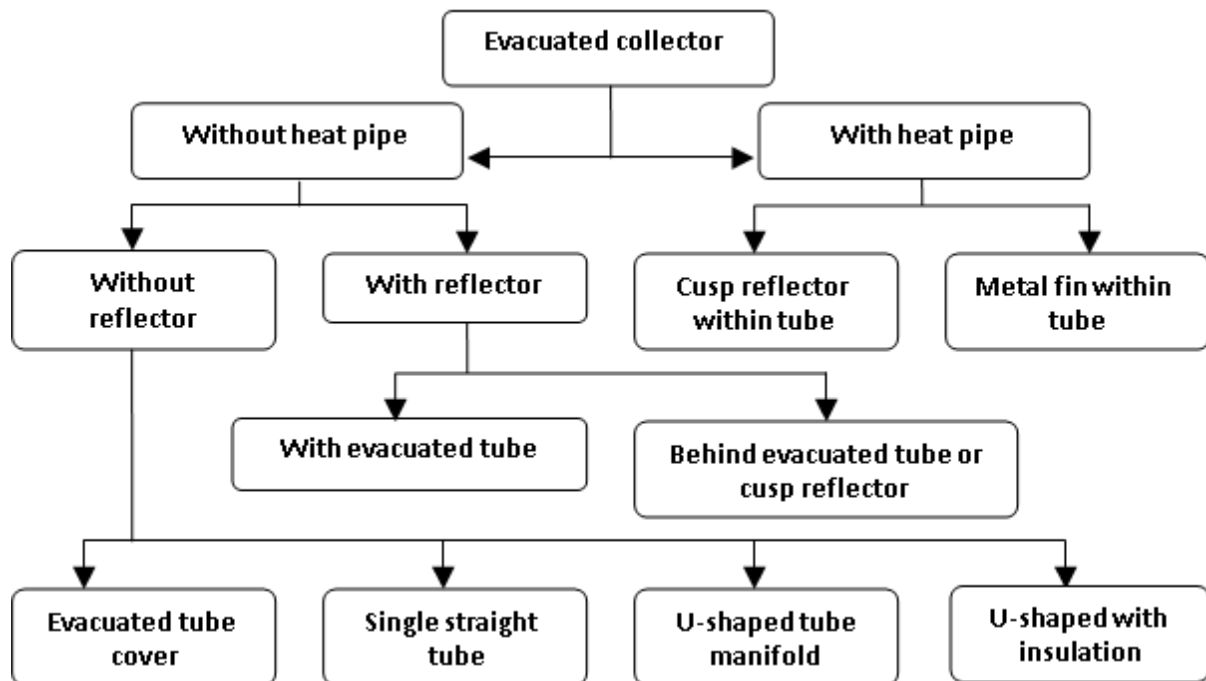


Figure I.7: Classification of an evacuated solar collector [12].

A heat pipe provides the most elegant way of extracting heat from an evacuated collector. Heat pipe is hermetically sealed tube that contains a small amount of liquid heat transfer. When one

portion of tube is heated, the liquid evaporates and condenses at the cold portion, transferring heat with great effectiveness due to the latent heat of condensation. The heat pipe contains a wick or to ensure that the liquid follows back to the heated portion repeating the cycle. It is easy to design a heat pipe (e.g., by giving it the proper tilt) so that it functions only in one direction. This thermal diode effect is very useful for the design of solar collectors because it automatically shuts down the collector and prevents heat loss when there is insufficient solar radiation. Also, heat pipes have lower heat capacity than ordinary liquid-filled absorber tubes, thus, minimizing warm-up and cool-down losses [10].

I.7.5 Concentrating collector

A concentrating collector utilizes a reflective parabolic-shaped surface to reflect and concentrate the sun's energy to a focal point or focal line where the absorber is located. To work effectively, the reflectors must track the sun. These collectors can achieve very high temperatures because the diffuse solar resource is concentrated in a small area [12].

The system may have a distributed or a central receiver. The concentrators may also be classified based on optical components. They may be reflecting or refracting type, imaging or non-imaging type, and line focusing or point focusing type. The reflecting of the refracting surface may be one piece or a composite surface; it may be a single or two-stage type system and may be symmetric or asymmetric. In practice. However, hybrid and multistage systems, incorporating various levels of features, occur frequently [13].

I.7.5.1 Line Focus Collectors

These collectors, sometimes known as parabolic troughs, are composed of parabolically shaped reflective sections connected into a long trough [14], use highly reflective materials to collect and concentrate the heat energy from solar radiation [15]. The pipe carrying water is placed in the center of this trough, hence, the collected sunlight is focused upon the pipe, heating the contents. These are very high-powered collectors and are generally used to generate steam for solar thermal power plants, but not used in residential applications. These troughs can be extremely effective in generating heat from the Sun, particularly those that can pivot, tracking the Sun to ensure maximum energy collection [14].

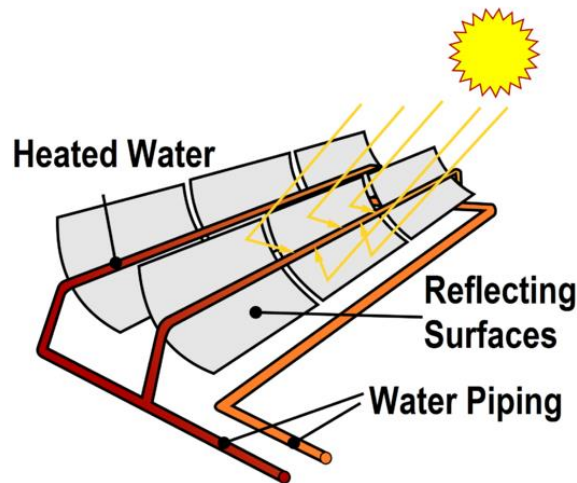


Figure I.8: A diagram of a line focus solar collector.

I.7.5.2 Point Focus Collectors

These collectors are large parabolic dishes composed of some reflective material that focuses the Sun's energy onto a single point. The heat from these collectors is generally used for driving Sterling engines [14]. Although very effective at collecting sunlight, they must actively track the Sun across. These dishes can be customized in one set or combined into an array to collect more energy [16].

Point focus collectors and similar apparatuses can also be utilized to concentrate solar energy for use with concentrated photovoltaics. Instead of producing heat, the Sun's energy is converted into electricity with high-efficiency photovoltaic cells, designed specifically to harness concentrated solar energy.



Figure I.9: A point-focus solar collector.

I.8 Advantages and disadvantages of solar power plant

I.8.1 Advantages of solar power plant

- These plants use the sun's energy, a readily available renewable resource that can be used to produce electricity without depleting finite resources like fossil fuels.
- Since there aren't many moving parts in them, the maintenance will drive a real cost saving.
- They do not produce emissions or pollutants, which helps to reduce the carbon footprint and improve air quality.
- These can be built and operated at a local level, reducing the need for long-distance transmission of electricity, neither a large voltage network, saving associated costs and avoid negative environmental impact.
- Recently, the cost of solar technology has been proved a decrease rate, making solar power plants an increasingly cost-effective option for generating electricity.

I.8.2 Disadvantages of solar power plant

- Due to their reliance on sunshine, these plants cannot produce power at night or during bad weather.
- Building a solar power plant can be an expensive initial investment, making it a less viable choice.
- They rely on batteries or other energy storage equipment to store the extra energy produced during periods of strong sunshine.
- The capacity and cost of these storage devices may vary.
- There can be a problem in places with little accessible space because they need large lands to install panels and auxiliary equipment.
- For the powerful MW required in some industrial needs, the solar power plant present a very weak alternative face to gas turbine or steam turbine power plants.

I.9 Application of solar collector

The solar collector is used in multiple domains such as:

- ❖ Solar Heating
- ❖ Solar Air Conditioning
- ❖ Solar drying
- ❖ Solar distillation
- ❖ Solar Desalination
- ❖ Solar cooling

I.10 conclusion

In this chapter, we saw the definitions and general basic concepts of solar energy, types of energy exchange, the different examples of solar collectors, and their application domains. Moreover; this chapter has shown that it is necessary to have a good knowledge of the properties of solar collectors to improve the thermal and dynamic performance of solar drying.

References

- [1] Ndiaye et al, UNIVERSITÉ CHEIKH ANTA DIOP DE DAKAR, THÈSE DE DOCTORAT, Spécialité THERMIQUE ÉNERGÉTIQUE ET ENVIRONNEMENT, « Optimisation des performances d'un capteur solaire à air et estimation des coefficients d'échange paroi-fluide », 2018. (Our translation)
- [2] Norton, Brian (2013-10-11). *Harnessing solar heat*. Dordrecht.
- [3] Rabl, Ari. (1985). *Active solar collectors and their applications*. New York: Oxford University Press.
- [4] Sreekumar, S.; Joseph, A.; Kumar C. S., S.; Thomas, S. (2020-03-10). "Investigation on the influence of antimony tin oxide/silver nanofluid on direct absorption parabolic solar collector". *Journal of Cleaner Production*.
- [5] G. Lefèbvre, La méthode modale en thermique: Modélisation, simulation, mise en oeuvre, applications, Ellipses, France, (2007). (our translation)
- [6] H. Soffar, Nov 2019. URL <https://www.online-sciences.com/the-energy>.
- [7] Benahmed et al, « Simulation numérique des transferts thermiques dans un capteur solaire plan à air à double passe », mémoire de master, Université Ibn khaldoun Tiaret, (2016).
- [8] Etude expérimentale d'un bassin d'eau utilisé comme capteur solaire plan présent Par Abdelaoui Med Khimmusti et GurichaFoud thème d'ingénieur d'état universitede Ouargla (our translation)
- [9] Yuwen Zhang, (13 July 2010) on the website Thermal Fluids Central.
- [10] Rabl A. *Active Solar Collectors and Their Applications*. – New York: Oxford University Press, 1985. – pp. 503.
- [11] Ramlow B., Nusz B. Types of Solar Collectors [online] [viewed 2007.11.25.]. Available: http://oikos.com/library/solarwaterheating/collector_types.html.

- [12] Tiwari G.N. Solar Energy. Fundamentals, Design, Modeling, and Applications. – New Dehli: Alpha Science International Ltd, 2006. – p. 525.
- [13] Žanis Jesko Latvia University of Agriculture, Faculty of Engineering Jelgava, “CLASSIFICATION OF SOLAR COLLECTORS” 29.-30.05.2008.
- [14] G. Boyle. Renewable Energy: Power for a Sustainable Future, 2nd ed. Oxford, UK: Oxford University Press, 2004.
- [15] US Department of Energy. (August 10, 2015). *Line Focus Solar Collector* [Online].
- [16] JC Solar Homes. (August 10, 2015). *Concentrators and Flat Plate Collectors* [Online].

Chapter II: Bibliographic Research

II.1 Introduction

Owing to the single-air flat solar collector's, inadequate capacity to produce enough heat for drying or other thermal applications. Numerous studies using a variety of numerical and experimental methods have been conducted to improve the thermal and dynamic performance of solar thermal collectors using a range of methods.

Thermal weakening results from a poor rate of heat transfer between the absorbent plate and air because of the unfavorable thermo-physical characteristics of air. Thus, a number of methods are employed to enhance the efficiency of heat exchangers for solar applications by raising the rate of heat transfer between the absorber and the air.

II.2 Research on single-pass solar collector

A. Ahmed-Zaid, and al (2001), [1] presented a comparison between the results obtained in the case of the solar collector with obstacles and the collector without obstacles (SC).

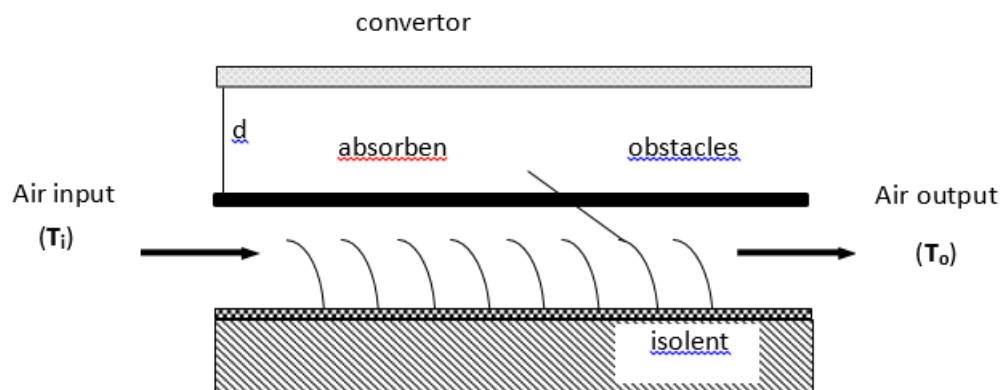


Figure II.1: Solar collector components.

The various forms studied (The different shapes), both simple and complex, concerning Delta baffles Longitudinally Cinched (DCL), Longitudinal Cinched Ovals (OCL), and Transversal-Longitudinal (TL).



Figure II. 2: Disposal of obstacles DCL.

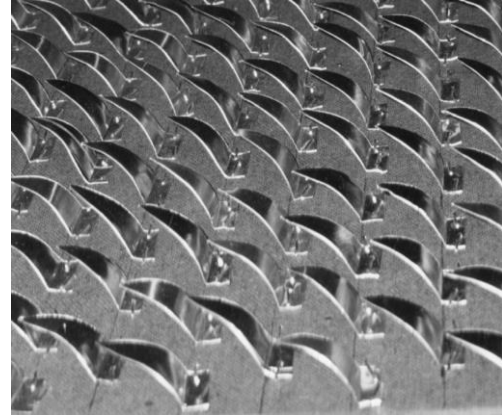


Figure II.3: Disposal of obstacles OCL.

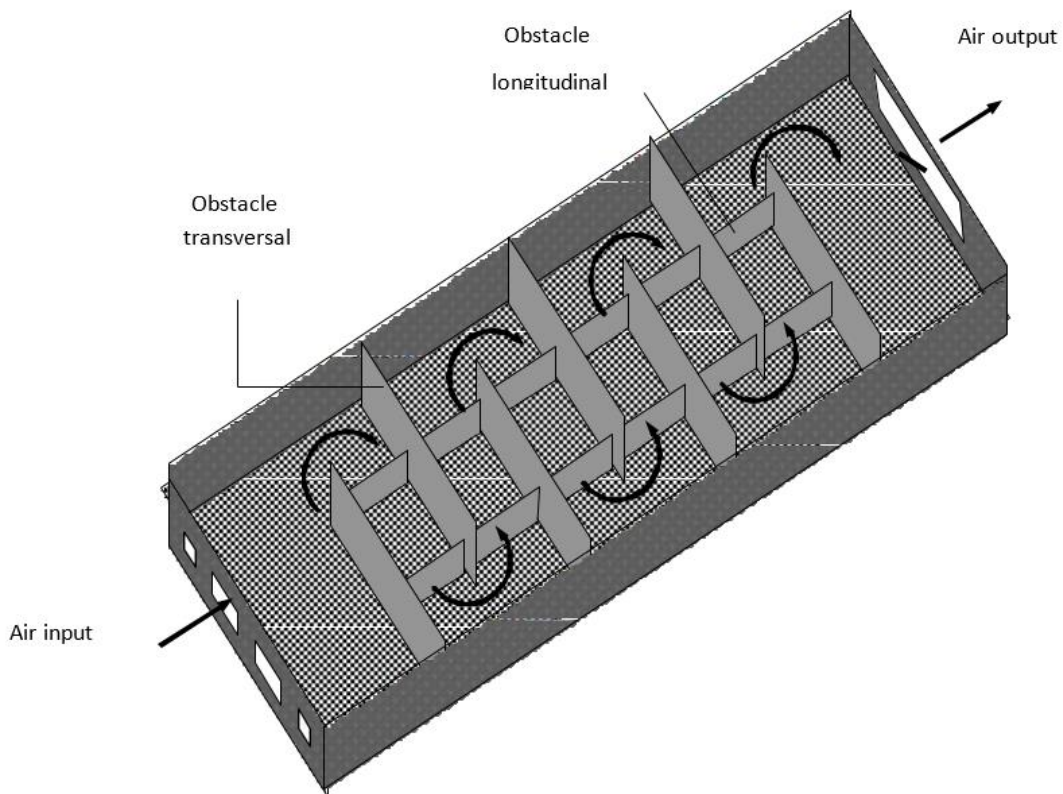


Figure II.4: collector with obstacles TL.

In this study, by simulating solar energy, we sought to improve the collector's "Performance-Temperature Difference" torque by introducing baffles (obstacles) which are deposited in the dynamic vein of the collector. Thermal transfers, output temperature, and collector's performance are significantly improved. An application of the best systems is presented to dry yellow onion and hareng in interesting times.

From their previous experience, they concluded that the baffles (DCL) are better than (OCL) however the baffles (TL) present a better yield than (DCL), moreover, (SC) gives us the minor yield among all.

Moummi, and al (2004), [2] created an increasingly turbulent flow between the absorber and the back wooden plate. For that, they used obstacles of various forms. In their study, they chose rectangular plate fins inserted perpendicular to the flow. The fluid flows out through the interstices between fins in the same row, this allows a good distribution of the fluid and reduces the dead zones. Secondly, and for the same configuration, they undertook a study on the evaluation of the transfer coefficient.

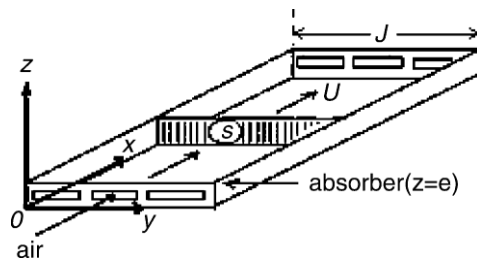


Figure II.5: Dandail in air channel duct.

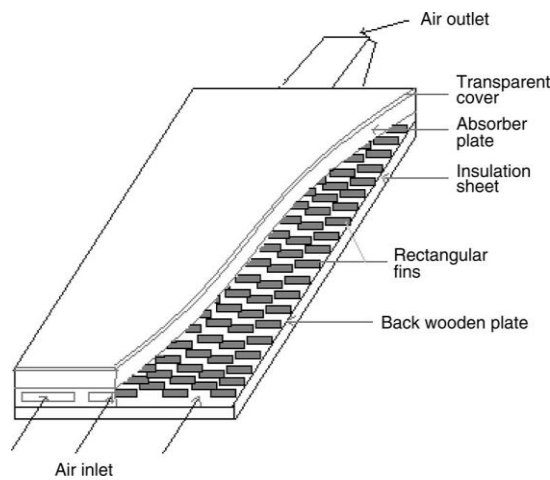


Figure II.6: Collector with finned system on the back wooden plate.

The results are compared with those obtained with a solar air collector without fins, using two types of absorbers selective (in coppersun) or not selective (black-painted aluminium).

K.Aoues, and al (2008), [3] a mathematical model that allows the determination of the single-pass solar air collector thermal performances is developed. The model can predict the temperature profile of all collector components and the air stream in the channel duct. Later on, the cylindrical roughness is introduced, which increases the thermal heat transfer between the absorber plate and the fluid. The cylindrical roughness, mounted in two configurations (Aligned and staggered rows), is oriented perpendicular to the fluid flow and they are placed underside of the absorber plate. They are characterized by high heat transfer area per unit volume and generate low-pressure losses.

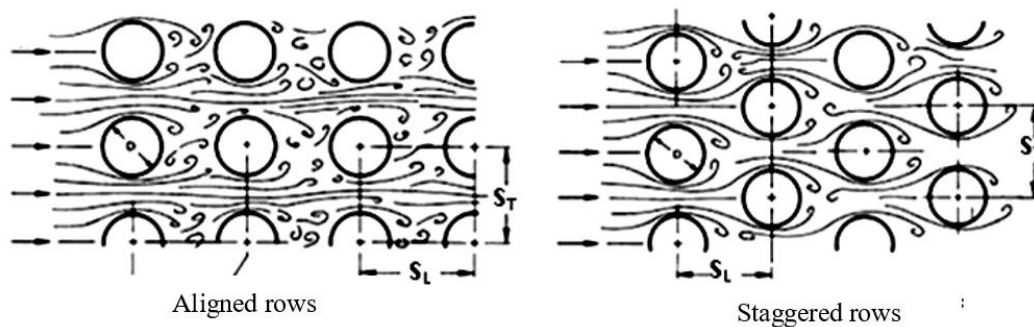


Figure II.7: Different positions of cylindrical roughness.

The results reflect the gain achieved by further artificial cylindrical-shaped roughnesses. The efficiency is much higher for a collector fitted with baffles in its mobile air vein than compared to the smooth collector.

K.Aoues, and al (2009), [4] executed an experimental investigation of the performance of a flat plate air solar collector outfitted with artificial roughness of different forms and different arrangements. A complete collector test facility equipped with a data acquisition system has been assembled and tested for this purpose. A flat plate solar collector, of 1.74 m² area has been designed and constructed. The adapted artificial roughness unit is structured from a fin-galvanized mandal. Four configurations with two forms (model-1 and model-2) of artificial

roughness and two arrangements (A and B) are combined (A1, A2, B1, and B2) and tested. The flat plate air solar collector was mounted on a stand facing south at an inclination angle, and they were tested in the environmental conditions. The experimental sand up was instrumented for the measurement of solar radiation, ambient temperature, outland and inland air temperature, air flow rate, and wind velocity. The comparison of the performance of the four configurations studied resulted in the choice of the B1 configuration (baffles model-1) as the one that achieved the best performance.

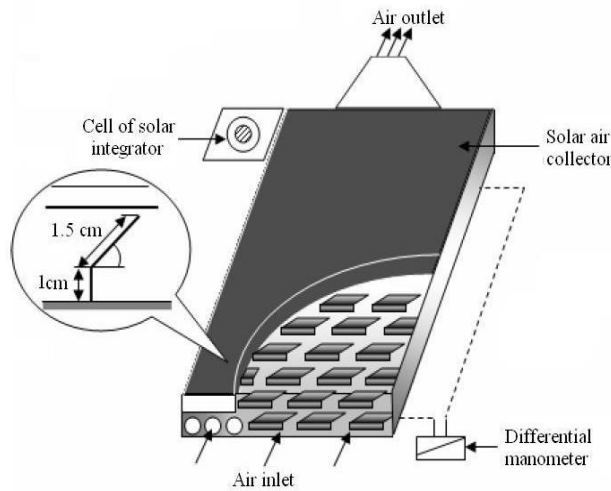


Figure II.8: The schematic of an experimental device.

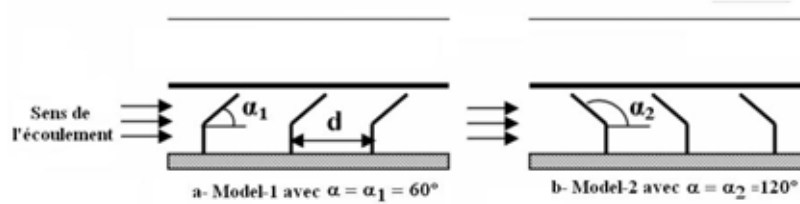


Figure II.9: a description of the baffle schematic

F. Chabane, and al (2018), [5] the thermal performance of a solar air heater is presented with additional fins. In their work, they developed an experimental study on the thermal performance of a solar collector air with and without a semi-cylindrical baffle. Trying to change the mass flow rate times for both configurations corresponding to tilt angle $\beta = 37^\circ$, it represented the optimum tilt angle related to the city of Biskra. The essential parameters are measurements of

the outland, an inland, and an ambient temperature and covering according to the influence of the wind velocity. Experiments on a solar collector designed for this purpose, have determined the thermal efficiency of solar collectors with and without semi-cylindrical baffles to different flow intervals to actually follow the evolution of the outland temperature of the air. The results provide the best thermal efficiency for the solar collector flat plate with a semi-cylindrical baffle is increased by 19% toward baffle less.

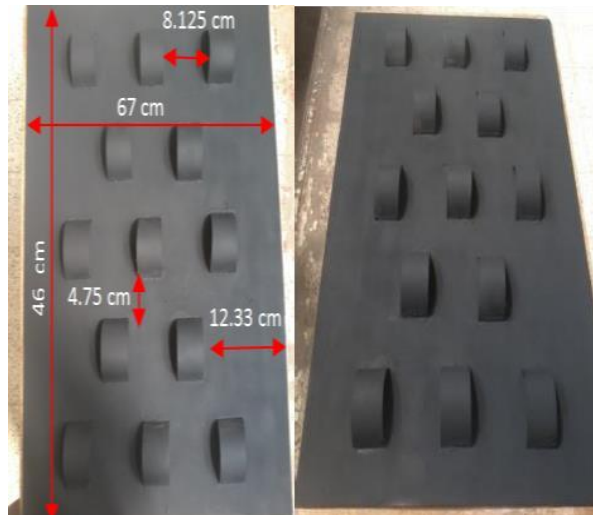


Figure II.10: Absorber with baffles in semi-cylindrical shape.

II.3 Research on double-pass solar collectors

K.Sopian, and al (1999), [6] presented the thermal performance of a double-pass solar collector with and without porous media in the second or lower channel of collector. The experimental sand up has been designed to study the thermal performance over a range of design and operating conditions. Several important relationships between the design and operating conditions have been obtained. These relationships affect the thermal performance of the double-pass solar collector. The relationships include the effect of changes in upper and lower channel depth on the thermal efficiency with and without porous media. Moreover, the effects of mass flow rate, solar radiation, and temperature rise on the thermal efficiency of the double-pass solar collector have been studied. The study concluded that the presence of porous media in the second channel increases the outland temperature, thus, increase the systems thermal efficiency.

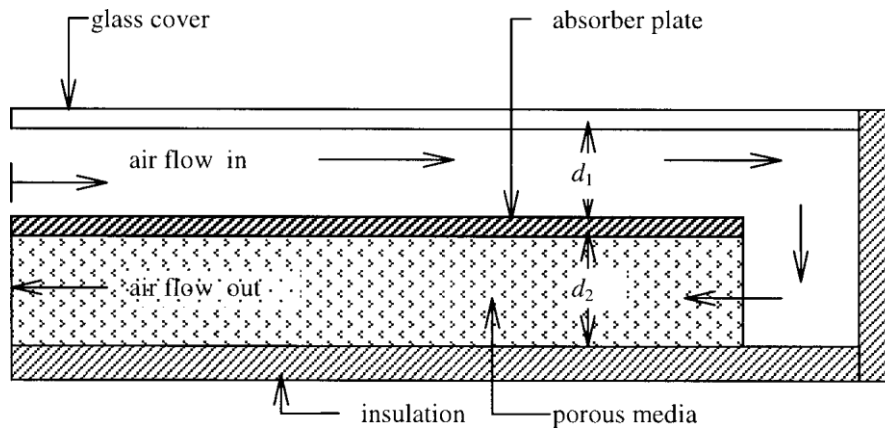


Figure II.11: The schematic of a double-pass thermal solar collector with porous media in the second channel.

E. A. Musa, and al (2004), [7] the study have been developed for air flowing through the porous media, which packed a double-pass solar air heater. Various porous media are arranged in different porosities to increase heat transfer, area density, and the total heat transfer rate. Transient heat transfer experiments indicate that both the heat transfer coefficient and the friction factor are strong functions of porosity. The heat transfer coefficient and the friction factor are also strong functions of the geometrical parameters of the porous media. A test collector was developed and conducted indoors by varying the design features and operating conditions using a halogen-lamp simulator as a radiation source. This type of collector can be used for drying and heat applications such as solar industrial processes, space heating, and solar drying of agricultural products.

Their results were compared with the experimental performance of the double-pass solar collector with and without porous media, and a favorable agreement was observed. The heat transfer coefficient increases by using more porous media in the lower channel of the double-pass solar collector.

P.Naphon (2005), [8] studied numerically the performance and entropy generation of the double-pass flat plate solar air heater with longitudinal fins. The mathematical models described the heat transfer characteristics of the double-pass flat plate solar air heater driven by the first thermodynamic principle (Energy conservation). The predictions are done at an

air mass flow rate ranging between 0.02 and 0.1 kg/s. The effects of the inland condition of working fluid and the dimension of the solar air heater on the heat transfer characteristics, performance, and entropy generation are considered.

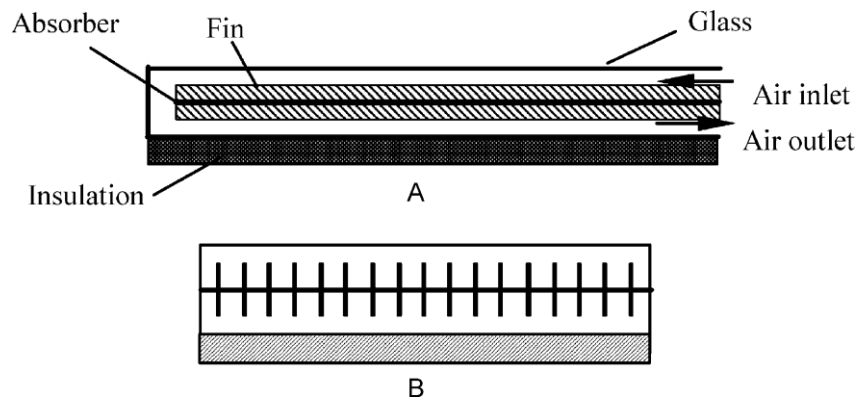


Figure II.12: Schematic diagram of the solar air heater.

P.Naphon found that the thermal efficiency increases with the number of fins, where the entropy of the system is inversely proportional to the number of fins.

Karim, and Hawlader (2006), [9] studied, flat plate, finned, and v-corrugated air heaters both experimentally and theoretically to improve the performance of conventional air heaters. Collectors were also tested in double-pass mode to investigate the extent of improvement in efficiency that could be achieved without increasing collector size or cost. A series of experiments were conducted, based on the ASHRAE standard, under the climatic conditions of Singapore. The performance of all three collectors was examined over a wide range of operating and design conditions. The v-corrugated collector was found to be the most efficient collector and the flat plate collector presented the lowest efficiency. Results showed that the v-corrugated collector is 10–15 and 5–11% more efficient in single-pass and double-pass modes, respectively, compared to flat plate collectors. The double pass operation of the collector improved the efficiency of all three collectors. The improvement in efficiency for the double pass mode was most significant in the flat plate collector and least in the v-groove collectors.

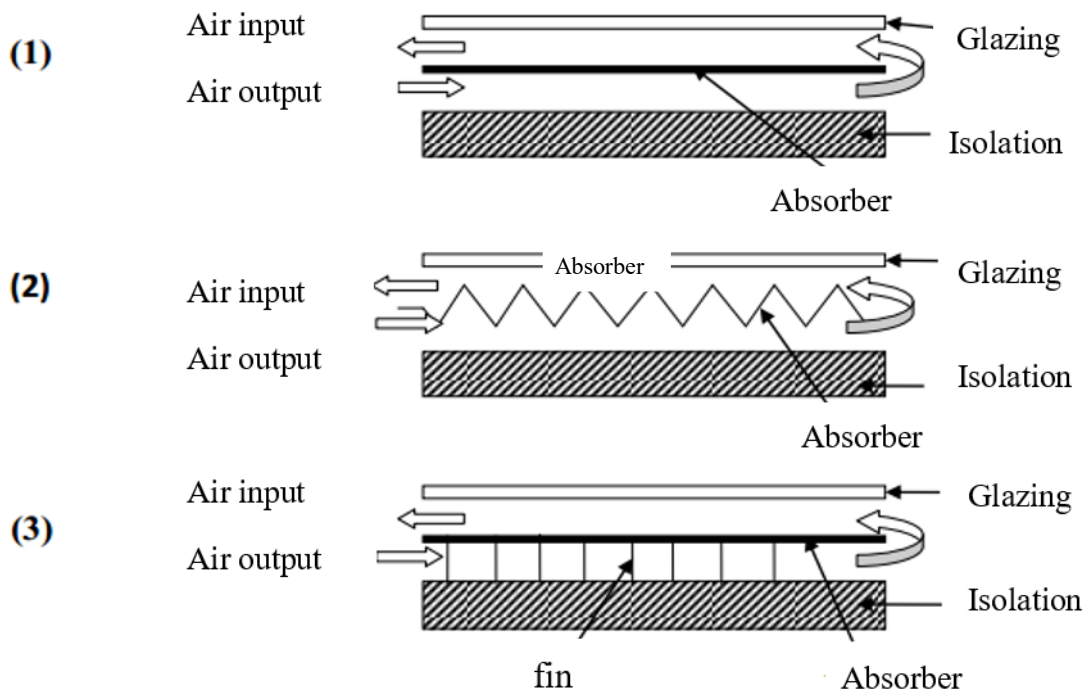


Figure II.13: flat plate (1), finned (2), and v-corrugated (3) air heaters.

C. Lertsatitthanakorn, and al (2008), [10] developed and tested a double-pass TE solar air collector. The TE solar collector was composed of transparent glass, an air gap, an absorber plate, thermoelectric modules, and a rectangular fin heat sink. The incident solar radiation heats the absorber plate so that a temperature gradient is created between the thermoelectric modules that generate a direct current. Only a small part of the absorbed solar radiation is converted to electricity, while the rest increases the temperature of the absorber plate. The ambient air flows through the heat sink located in the lower channel to gain heat. The heated air then flows to the upper channel where it receives additional heating from the absorber plate. Improvements to the thermal and overall efficiencies of the system can be achieved by the use of the double pass collector system and TE technology.

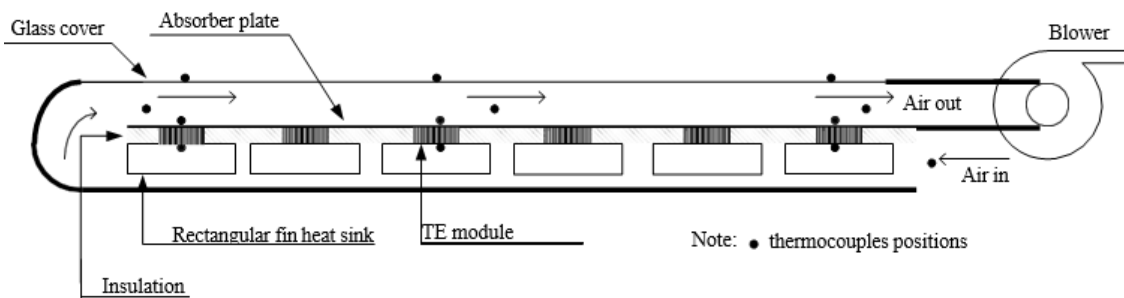


Figure II.14: A schematic diagram of the TE solar air collector.

C. Lertsatitthanakorn and al results show that the thermal efficiency increases as the airflow rate increases. Meanwhile, the electrical power output and the conversion efficiency depended on the temperature difference between the hot and cold sides of the TE modules. At a temperature difference of 22.8 °C, the unit achieved a power output of 2.13 W and a conversion efficiency of 6.17%. Therefore, the proposed TE solar collector concept is anticipated to contribute to wider applications of the TE hybrid systems due to the increased overall efficiency.

S.S. Krishnananth, and al (2012), [11] In this study, a double-pass solar air heater was fabricated and integrated with the thermal storage system. Paraffin wax is used as a thermal storage medium. The performance of this heater was studied for different configurations. The solar heater integrated with thermal storage delivered comparatively high temperatures. The efficiency of the air heater integrated with thermal storage was also higher than the air heater without a thermal storage system.

The study promotes the thermal storage medium at the absorber plate as the best configuration.

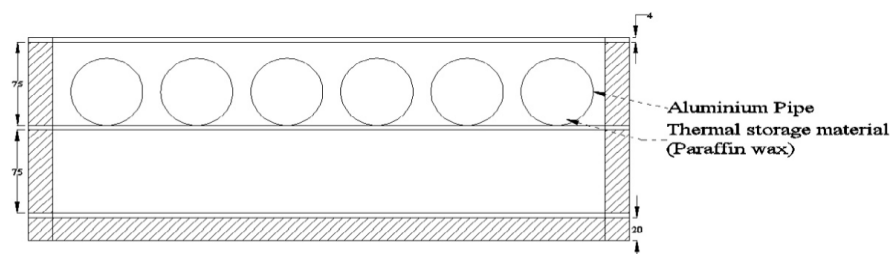


Figure II.15: Configuration 2, capsules above the absorber plate.

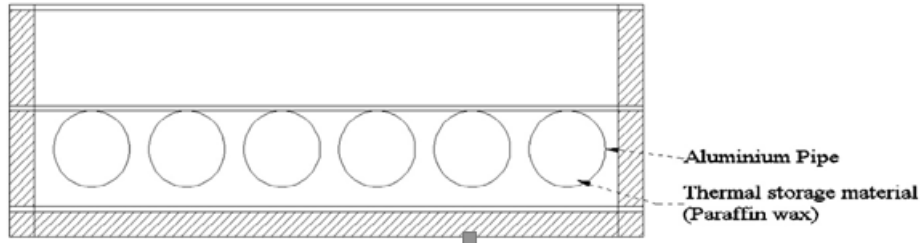


Figure II.16: Configuration 3, capsules below the absorber plate.

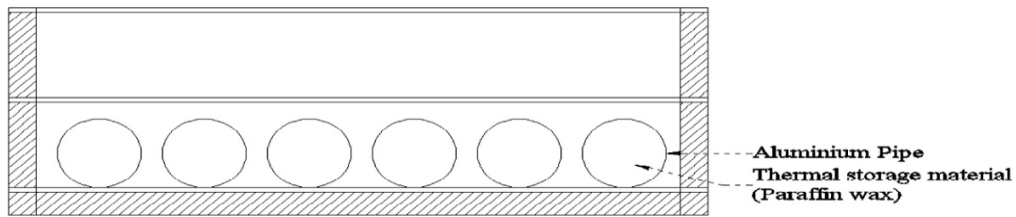


Figure II.17: Configuration 4, capsules above the back plate.

M. Sandali, A.N. Korti (2014), [12] a digital thermal transfer simulation of a double-pass solar air collector with and without a porous environment was performed. The porous environment, with different porosities, was placed in the lower channel of the solar collector. A comparison of two double-pass solar air collectors has been developed, with and without a porous environment. A thermal study was conducted on the effects of solar radiation gradient.

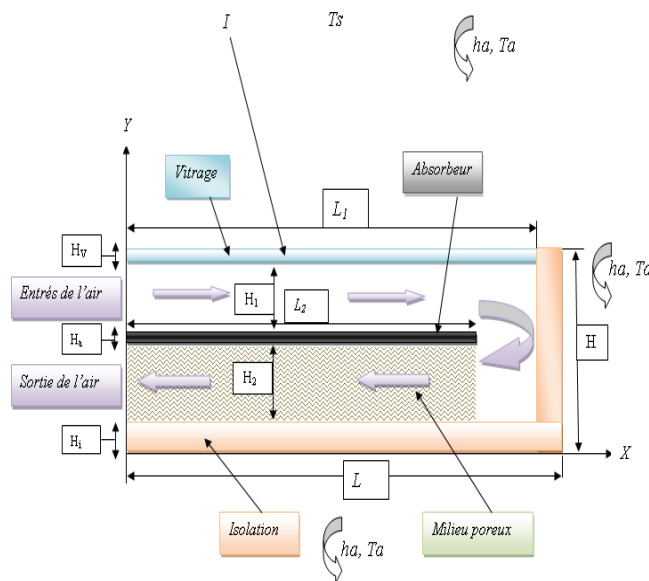


Figure II.18: double-pass solar collector with porous environment.

It is noted that the temperature of the fluid increases with solar irradiation. When the absorber uptake more heat with the elevation of solar radiation, its temperature becomes higher and increase the temperature of the fluid in upper and lower channels. As a result, the fluid temperature gap between the input and output of the solar collector increases.

Air temperature in the case of the solar collector with a porous environment is higher than in porous environment with no pores. So, it is observed that with the increase of solar radiation, the temperature increases in, the fluid at the output of the solar collector, and the difference in fluid temperature between the inlands/outland with and without a porous environment in the solar collector.

A.Labed, and al (2015), [13] in this work, they presented an extensive comparative study on the thermal performance and pressure drop of various designs of solar air heaters. thus, they proposed three technological solutions, i) adding different forms of obstacles in the air flow duct, ii) reversing the flow direction (blowing up / blowing down, iii) rotating the flow around the bottom plate to obtain a double pass flat plate collector having a trapezoidal obstacle. Thus, we have proceeded to the comparison of the seven models to determine the best-performing system.

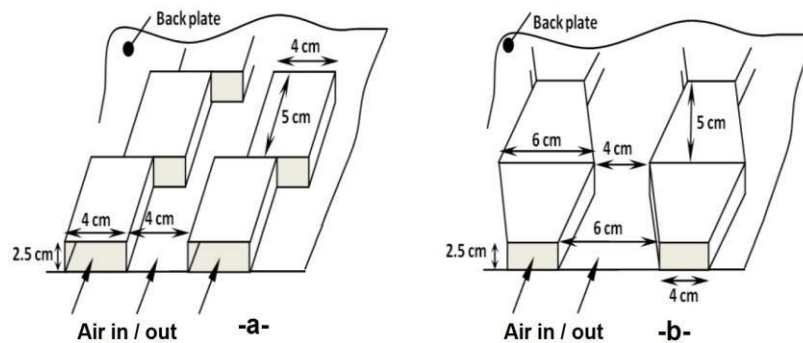


Figure II.19: schematics of different used obstacles.

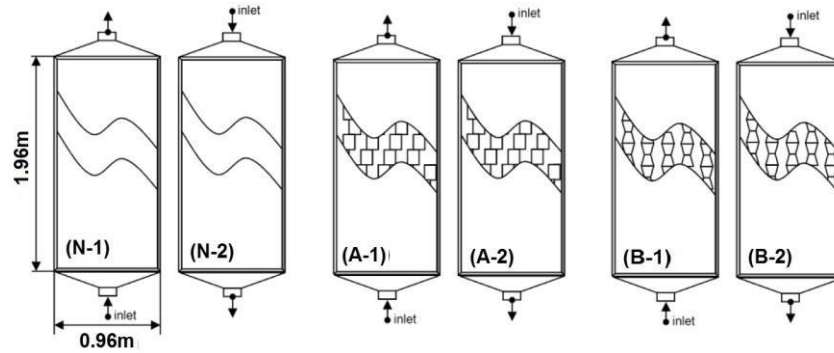


Figure II.20: the sixth studied model (N) without obstacles, (A) with rectangular obstacles, and (B) with trapezoidal obstacles.

It appears from the recorded values that the addition baffles, of trapezoidal shape with a normal incidence on the flow and for the case of the selected configuration and layout, seems the most advantageous compared to the rectangular baffles, hence, in both cases, the collector performance is significantly higher compared to a collector without baffles, an improvement of 15% for a flow rate of 80 m³/h is noted for a collector fitted with trapezoid baffles, and that for example to have a 50 % efficiency with a collector with no baffles, the required flow rate is of 75 m³ / h, whereas with a collector fused with trapezoidal baffles, the flow rate required is only 45 m³/ h.

Kalaiarasi, and al (2016), [14] presented an experimental energy and exergy analysis a novel flat plate solar air heater (SAH). It has a specially designed absorber plate made up of copper strips (copper tubes with extended copper fins on both sides), welded longitudinally to each other. In their study of the impact of this novel design and the sensible heat storage over the performance of the SAH, their results were compared with the output of a conventional SAH of similar dimensions. For the precise comparison of their performances, the experiments were conducted on both the SAHs at the same location, simultaneously. Experiments were conducted for two different mass flow rates (0.018 kg/s, and 0.026 kg/s). Their results showed that the maximum energy and exergy efficiency obtained was in the range of 49.4–59.2% and 18.25–37.53% respectively, for the SAH with sensible storage at $Q_m = 0.026$ kg/s. Besides, the SAH with sensible heat storage was observed to perform better than the conventional flat plate SAH without storage.

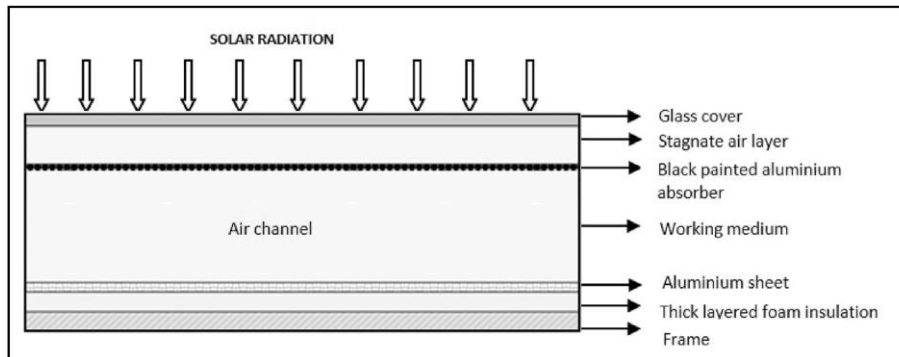


Figure II.21: Cross-sectional view of type-I SAH.

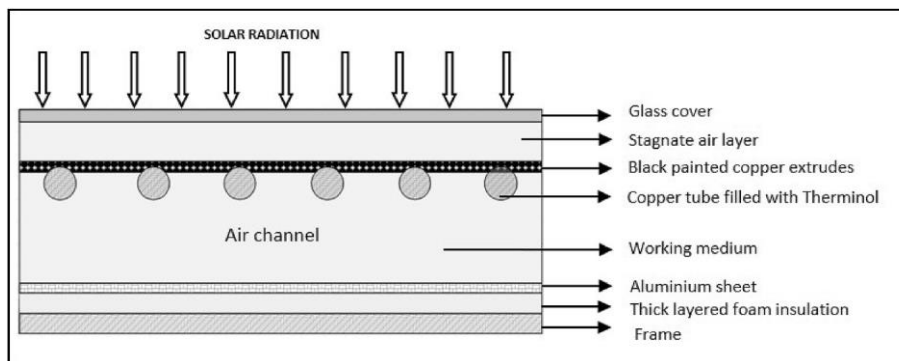


Figure II.22: Cross-sectional view of type-II SAH.

M. Nadia, and al (2018), [15] presented the study of a double-pass air insulated by crushed milland stem mixed with gum arabic. The study is carried out based on mathematical models obtained by writing energy conservation laws in the various components of the system, which made it possible to determine the evolution of the air temperature as a function of the length of the absorber, making a comparison with the experimental results. After comparing the results obtained with those found in the literature, the influence of some physical and geometrical parameters on the performance of the solar thermal collector is presented.

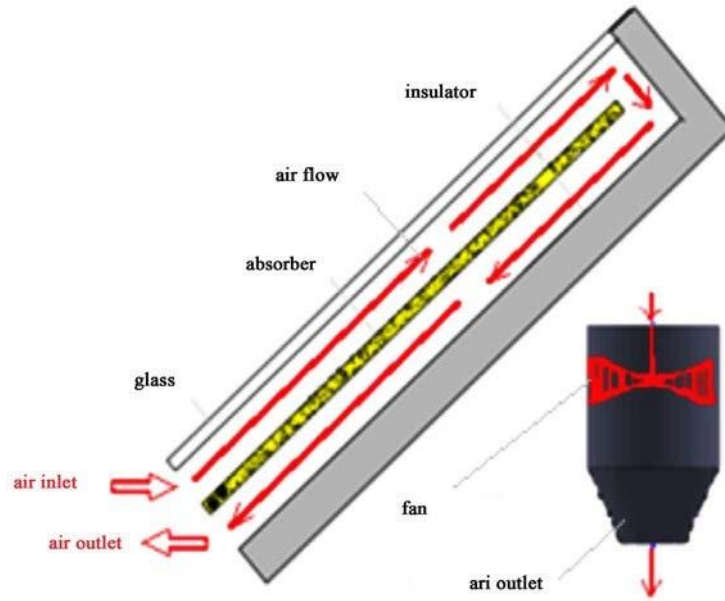


Figure II.23: Diagram of the studied solar collector.

Their results show a significant difference due to the lateral thermal losses, and also of the thermal inertia of the insulation material of the solar collector that are not taken into account in our global model.

II.4 Conclusion

Through the use of this bibliographic research, it has become clear that earlier researchers conducted a great deal of research and studies on solar air collectors. They have found many results that allow to improve the thermal efficiency and maximize the energy production of these collectors from the improvement of the different parameters having an influence on heat exchange efficiency.

This focuses on the analysis of thermal performance on the performance of flat solar collectors.

References

- [1] A.A. Zaïd, A. Moulla, M.S. Hantala and J.Y. Desmons. "Amélioration des Performances des Capteurs Solaires Plans à Air: Application au Séchage de l'Oignon Jaune et du Hareng". *Rev. Energ. Ren.* Vol.4 (2001) 69-78, (our translation).
- [2] N. Moummi, S. Youcef-Ali, A. Moummi and J. Y. Desmons, Energy analysis of a solar air collector with rows of fins, *Renewable Energy*, vol. 29 13, pp. 2053-2064, (2004).
- [3] K. Aoues, N. Moummi, M. Zellouf, A. Moummi, A. Labed and, E. Achouri, Andude de l'influence des rugosités artificielles sur les performances thermiques des capteurs solaires plans à air : Andude expérimentale dans la région de Biskra, *Revue des Energies Renouvelables Vol. 11 N°2 (2008) 219 – 227*.
- [4] K. Aoues, N. Moummi, M. Zellouf, A. Moummi, A. Labed, E. Achouri and, A .Benchabane, Amélioration des performances thermiques d'un capteur solaire plan à air: Andude expérimentale dans la région de Biskra, *Revue des Energies renouvelables*, vol. 12 2,pp. 237-248, (2009).
- [5] F.Chaaban, N.Moummi,A. Brima, «Experimental study of thermal efficiency of a solar air heater with an irregularity element on absorber plate », international journal of heat technology, vol. 36, no.3, september, 2018, pp.855-860.
- [6] K. Sopian, Supranto, W.R.W. Daud, M.Y. Othman,V.B. Yatimc. "Thermal performance of the double-pass solar collector with and without porous media". *Renewable Energy* 18 (1999) 557±564.
- [7] Musa, E.A., Sopian, K. and Abdullah, S. (2004) Heat Transfer Analysis and Pressure Drop Correlations for the Double-Pass Solar Collector with Porous Media. *Journal of Energy & Environment*, 3, 15-24.
- [8] Paisarn, 2005, On the performance and entropy generation of the double-pass solar air heater with longitudinal fins. *Renewable Energy*, 30(9), 1345-1357.
- [9] Karim and Hawlader, « Performance evaluation of a v-groove solar air collector for drying applications», *Applied Thermal Engineering* 26 (1) : 121-130. Scholar Bank@NUS Repository.2006.

[10] C. Lertsatitthanakorn and al, « Performance analysis of a double-pass thermoelectric solar air collector », *Solar Energy Materials and Solar Cells*, 92(9), 1105-1109, article (author version), 2008-09.

[11] S.S. Krishnananth, K.K. Murugavel. "Experimental study on double pass solar air heater with thermal energy storage". *Journal of King Saud University-Engineering Sciences* (2012).

[12] M. Sandali #1, A.N. Korti #2#, “ Laboratoire ANDAP”, Département de Génie Mécanique, Université de Tlemcen.

[13] A. Labed, N. Moumami, A. Benchabane, K. Aoues and M. Zellouf, « Performances thermiques et pertes de charges de différentes configurations de capteurs solaires plans à air Andude expérimentale dans la région de Biskra, Algérie » *Revue des Energies renouvelables*, vol. 18 2,pp. 209-216, (2015).

DOI: <https://doi.org/10.54966/jreen.v18i2.498>

[14] Kalaiarasi and al.2016, Experimental energy and exergy analysis of a flat plate solar air heater with a new design of integrated sensible heat storage. *Energy*, *III*, 609-619.

[15] M. Ndiaye, B. Diallo, S. Abboudi, D. Azilinson “Theorandical and Experimental Study of a Double Air-Pass Solar Thermal Collector with an Insulating Rod of Milland” *Energy and Power Engineering*, 2018, 10, 106-119.

<http://www.scirp.org/journal/epe>

Chapter III: Mathematical formulation and numerical modeling

III.1 Introduction

In this chapter, we presented the mathematical model adopted to characterize the flow and heat transfer of air by convection in a turbulent and stationary mode in the conduit of a single-pass solar air collector. However, we specified the limits conditions of this problem, in order to highlight the various mathematical equations as well as numerical approaches that have been used to analyze the movement of air and heat transfer within a collector.

III.2 Main methods of discretion

The transition to continuous partial derivatives to a discrete problem, relies on the standard methods of numerical analysis. There are three main methods for formulating a continuous problem in discrete form, the finite differences method, finite elements method, and finite volumes method. The method used by the "ANSYS FLUENT" code is the finite volumes.

III.2.1 Finite deference

The calculation field is discretized into a finite number of points, on which Taylor series developments are reduced in the selected precision order approach of the model equation derivative operators.

III.2.2 Finite elements

The fundamental principle of the finite element method is to divide the area of study into finite-dimensional elementary areas. In each of these domains, called finite elements, the unknown function is approached by a polynomial whose degree may vary from application to application but is generally low. These elements, triangles or quadrilateral, rectilinear or curvilinear, must make a partition of the area of study (they are disjointed and their union covers the entire area). This partition, which is commonly referred to as cutting or discretizing the domain, must comply with several rules to ensure that the calculation proceeds smoothly.

III.2.3 Finite volume method

The finite volume method (MFV) is a numerical approach that converts partial derivative equations, which express the laws of conservation, into discrete algebraic equations applied to finite volumes, also called cells, rather than to differential volumes. It was initially implemented by McDonald's to simulate a two-dimensional drain. The fundamental concept of the finite volume method is the subdivision of the calculation area into a set of elementary

volumes that surround the mesh points. The differential equation governing the problem is integrated into each control volume, which ensures preservation principles near the points or nodes of the discrete mesh. The result translates into a discretization equation, contains the values in the area studied.

The different stages of the finite volume method are:

- The discretization of the domain is considered in control volume.
- Integration of differential equations with partial derivatives.
- Writing algebraic equations of the mesh nodes.
- Resolution of the linear algebraic system obtained.

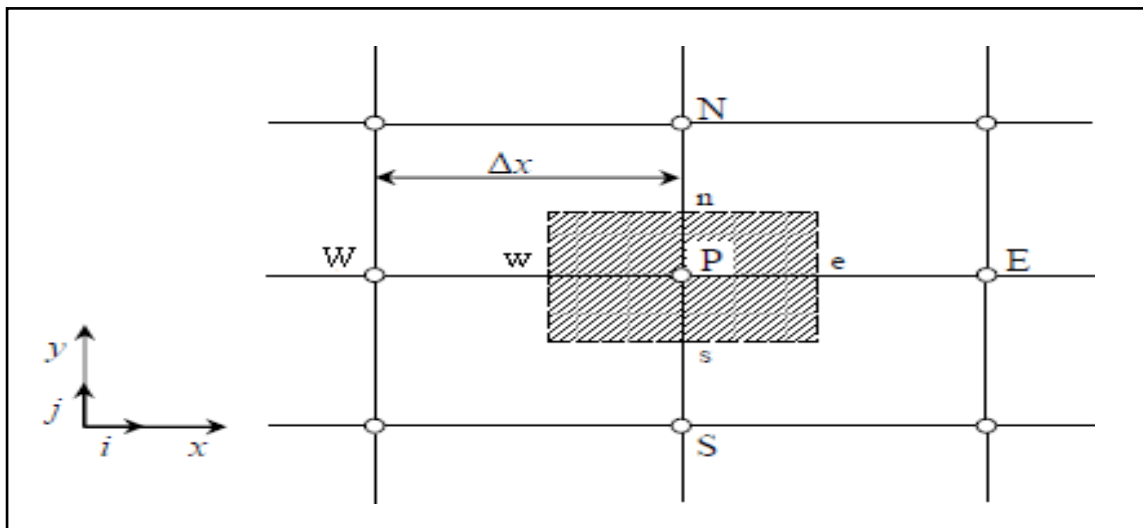


Figure III.1: Two-Dimensional Control Volume [1].

The control volume is shown in Figure III.1, For a main node P, the points E and W (East and West) are neighbors in the x direction, while N and S (North and South) are those in the y direction. The control volume surrounding P is shown by the discontinuous lines. The sides of the control volume are located at point(s) and W in the x direction, and n and s in the y direction [1].

$$\underbrace{\frac{\partial}{\partial t}(\rho\varphi)}_{\mathbf{T}} + \sum_{j=1} \underbrace{\frac{\partial}{\partial x_j}(\rho u_j \varphi)}_{\mathbf{C}} = \sum_{j=1} \underbrace{\frac{\partial}{\partial x_j} \left(\Gamma \varphi \frac{\partial \varphi}{\partial x_j} \right)}_{\mathbf{D}} + \underbrace{S_\varphi}_{\mathbf{S}} \quad (\text{III.1})$$

With:

T: Transitional Term;

C: Convective Term;

D: Broadcast Term;

S: Source Term.

We have just seen that, for each variable φ , the transport equation is written in the two-dimensional stationary case [1].

$$\frac{\partial}{\partial x}(\rho u \varphi) + \frac{\partial}{\partial y}(\rho v \varphi) = \frac{\partial}{\partial x} \left(\Gamma \frac{\partial \varphi}{\partial x} \right) + \frac{\partial}{\partial y} \left(\Gamma \frac{\partial \varphi}{\partial y} \right) + S_\varphi \quad (\text{III.2})$$

Where:

φ Is the carried property, Γ indicates the diffusion coefficient, and S_φ the source term.

III.3 Governing Equations

The solution of a fluid mechanics or energy problem takes place in the following steps: For each particle, we first have to start from the equations governing the movement, and then we will have to add the conditions to the limits and the initial conditions.

Then it will be a matter of choosing a resolution method. The final step is to define the flow characteristics through a treatment station to have the physical characteristics of the flow (heat transfer, flow, forces, separation, and attachment). For a general variable (φ), the conservative form for all flow transport equations can be written as follows [2]:

$$\frac{\partial(\rho\varphi v)}{\partial t} + \text{div}(\rho\varphi v) = \text{div}(\Gamma \text{grad}\varphi) + S_\varphi \quad (\text{III.3})$$

This equation is used as a basis for all CFD methods, in particular, the finite volume method, where the key step in this method is to integrate the equation (III.5) onto a control volume.

Then we get the following form:

$$\int \frac{\partial(\rho\varphi)}{\partial t} dV + \int \text{div}(\rho\varphi v) dV = \int \text{div}(\Gamma \text{grad}\varphi) dV + \int S_{\varphi} dV \quad (\text{III.4})$$

Using the Gauss divergence theorem, the equation (III.3) becomes:

$$\frac{\partial}{\partial t} \int \rho\varphi dV + \oint \rho\varphi v dA = \int \Gamma \nabla \varphi dA + \int S_{\varphi} dV \quad (\text{III.5})$$

The above equation is the general transport equation and can be easily converted into an energy flow equation by the general variable (φ) with:

(φ) = 1, which will give the continuity equation.

(φ) = u, which will give the equation of the quantity of movement following the x-axis.

(φ) = v, which will give the equation of the quantity of movement following the y-axis.

(φ) = w, which will give the equation of the quantity of movement following the z-axis.

(φ) = T, which will give the energy equation.

Indeed, by taking the values of (φ) and choosing appropriate values for the diffusion coefficient (Γ), and the source term, we obtain the mathematical formulation governing the movement of the fluid. The phenomenon of forced convection is based on the equations that bind the different parameters, namely: speed, pressure, and temperature. These equations are obtained from:

- mass conservation Law (continuity equation)

This equation is driven by the first principle of mass conservation. It is expressed mathematically in the following form:

$$\frac{\partial U}{\partial X} + \frac{\partial V}{\partial Y} + \frac{\partial W}{\partial Z} = 0 \quad (\text{III.6})$$

- the law of motion quantity conservation (Navier-Stokes equation)

This equation is derived from the dynamics second law, which states that the change in the amount of movement of a fluid particle is equal to the sum of the external forces on that particle. It is written in the form:

Following the axis (OX)

$$\frac{\partial(UU)}{\partial X} + \frac{\partial(VU)}{\partial Y} + \frac{\partial(WU)}{\partial Z} = -\frac{1}{\rho} \frac{\partial P}{\partial X} + \left[\frac{\partial}{\partial X} \left(\frac{\partial U}{\partial X} \right) + \frac{\partial}{\partial Y} \left(\frac{\partial U}{\partial Y} \right) + \frac{\partial}{\partial Z} \left(\frac{\partial U}{\partial Z} \right) \right] \quad (\text{III.7})$$

Following the axis (OY)

$$\frac{\partial(UV)}{\partial X} + \frac{\partial(VV)}{\partial Y} + \frac{\partial(WV)}{\partial Z} = -\frac{1}{\rho} \frac{\partial P}{\partial Y} + \left[\frac{\partial}{\partial X} \left(\frac{\partial V}{\partial X} \right) + \frac{\partial}{\partial Y} \left(\frac{\partial V}{\partial Y} \right) + \frac{\partial}{\partial Z} \left(\frac{\partial V}{\partial Z} \right) \right] \quad (\text{III.8})$$

Following the axis (OZ)

$$\frac{\partial(UW)}{\partial X} + \frac{\partial(VW)}{\partial Y} + \frac{\partial(WW)}{\partial Z} = -\frac{1}{\rho} \frac{\partial P}{\partial Z} + \left[\frac{\partial}{\partial X} \left(\frac{\partial W}{\partial X} \right) + \frac{\partial}{\partial Y} \left(\frac{\partial W}{\partial Y} \right) + \frac{\partial}{\partial Z} \left(\frac{\partial W}{\partial Z} \right) \right] \quad (\text{III.9})$$

- The law of Energy Conservation(energy equation)

The energy equation is obtained by applying the thermodynamics first principle to an incompressible Newtonian fluid, it is written as follows:

$$\rho C_p \left[\frac{\partial(UT)}{\partial X} + \frac{\partial(VT)}{\partial Y} + \frac{\partial(WT)}{\partial Z} \right] = \left[\frac{\partial}{\partial X} \left(K \frac{\partial T}{\partial X} \right) + \frac{\partial}{\partial Y} \left(K \frac{\partial T}{\partial Y} \right) + \frac{\partial}{\partial Z} \left(K \frac{\partial T}{\partial Z} \right) \right] + q \quad (\text{III.10})$$

Where C_p is the specific heat and ρ is the air density.

III.4 Closure Templates

They're equations that complement balance equations. In our case, it is about closing the general model by modeling the turbulent viscosity term and the Reynolds tensions term.

"ANSYS FLUENT" provides the following turbulence pattern choices:

- ❖ Spalart-Allmaras model.

- ❖ $k-\varepsilon$ models.
- ❖ Standard $k-\varepsilon$ model.
- ❖ Renormalization-group (RNG) $k-\varepsilon$ model.
- ❖ Realizable $k-\varepsilon$ model.
- ❖ $k-\omega$ model.
- ❖ Standard $k-\varepsilon$ model.
- ❖ Shear-stress transport (SST) $k-\varepsilon$ model.
- ❖ $v^2-\rho$ model.
- ❖ Reynolds stress model (RSM).
- ❖ Detached eddy simulation (DES) model.

Large eddy simulation (LES) model [3]. Among these models, there is a $(k-\varepsilon)$ stand that we will use in our simulation.

III.4.1 $(k-\varepsilon)$ Model

It is a model with two transport equations for two turbulence parameters. Using the analogy between the exchange of quantity of movement by molecular interaction on a micro-scale level (viscous constraints) and the exchanges of quantities of motion by turbulence in a micro-scale level (constraints de Reynolds). The idea of the model $(k-\varepsilon)$ is that one can construct from these quantities a "turbulent viscosity proper to the flow", where the turbulent viscosity is given by the following ratio:

$$V_1 = C_\mu \left(k^2 / \varepsilon \right) \quad \text{(III.11)}$$

With:

$$\mu_1 = \nu_1 \rho \quad \text{(III.12)}$$

Turbulent dynamic viscosity Experience shows that this relationship is well verified for flows to a large number of Reynolds provided they have a homogeneous turbulence.

C_μ : Non-dimensional coefficient that needs to be evaluated experimentally

K : The kinetic energy of turbulence is defined by:

$$k = 1/2 \overline{u_t^2} = 1/2 \left(\overline{u_1^2} + \overline{u_2^2} + \overline{u_3^2} \right) \quad (\text{III.13})$$

ε : The dissipation rate of kinetic energy turbulence is given by:

$$\varepsilon = \nu \left[\frac{\partial w}{\partial x_j} \right]^2 \quad (\text{III.14})$$

This term of dissipation that appears in the turbulent kinetic energy equation remains to be determined. The typical length scale of large turbulence structures is derived from:

$$\varepsilon = k^{3/2} / l \quad (\text{III.15})$$

➤ Model (k- ε) Standard Constants

To make the system of equations operational we adopt the standard constants of the model given by Launder and Spalding (1974). They are summarized in the following table:

C_μ	$C_{\varepsilon 1}$	$C_{\varepsilon 2}$	δK	$\delta \varepsilon$
0.09	1.44	1.92	1.0	1.0

Table III.1: Standard K-S model coefficients.

III.5 ANSYS FLUENT definition

ANSYS FLUENT is a general-purpose computational fluid dynamics (CFD) software used to model fluid flow, heat, and mass transfer, chemical reactions, and more. ANSYS FLUENT offers a modern, user-friendly interface that streamlines the CFD process from pre- to post-processing within a single window workflow.

III.6 Problem Geometry

A frame with a sealing material. On the underside of the rectangular box, insulation consisting of four layers: a 2 mm thick wooden plate, a 2 mm thick glass wool layer, a 40 mm thick polystyrene sheet, and a 1 mm thick wooden plate on which a 2 mm thick aluminum sheet was painted matte black and used to absorb the incident solar radiation.

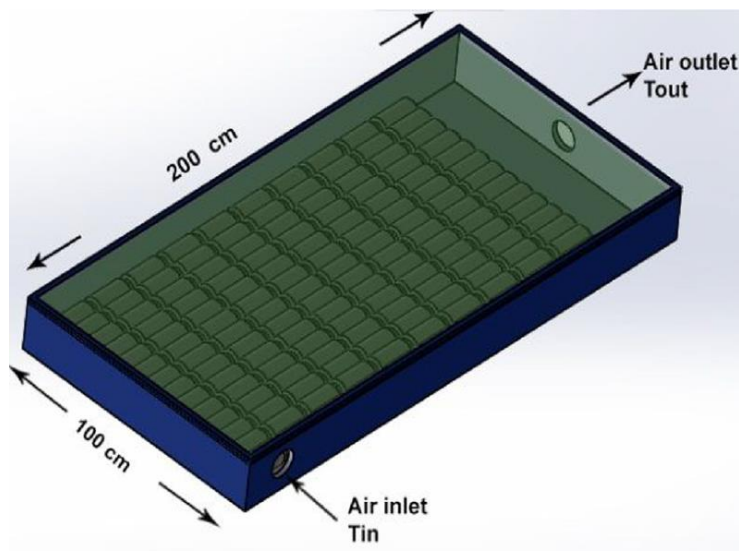


Figure III.2: Schematic representation of a solar air collector [4].

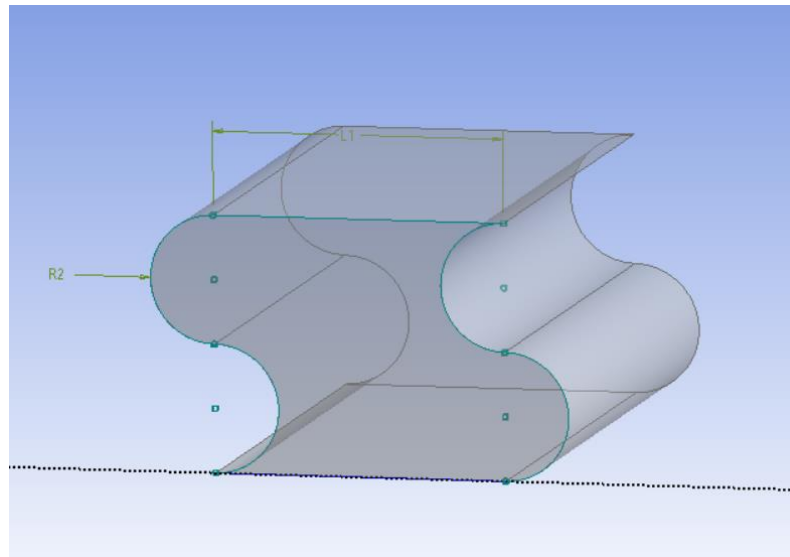


Figure III.3: schematic of the baffles used in the solar collector.

A baffle is an obstacle placed in a flow path to deflect or slow the flow. In a solar thermal collector, a baffle can be used to improve heat transfer by directing the flow of heat transfer fluid over the absorber plate more evenly.

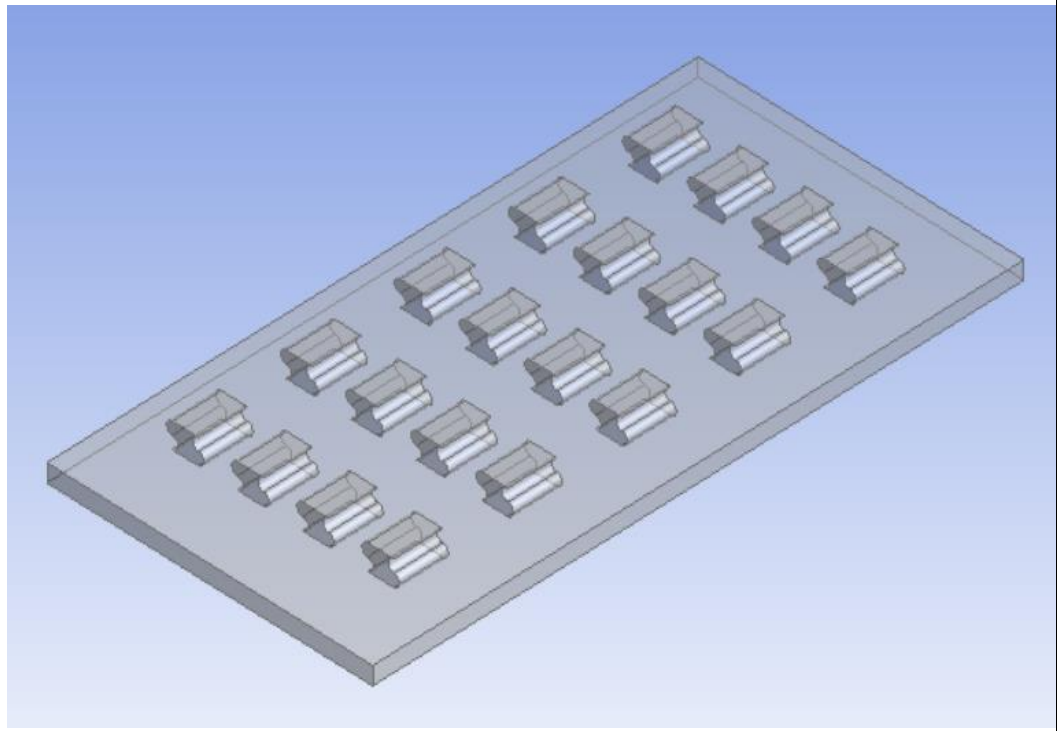
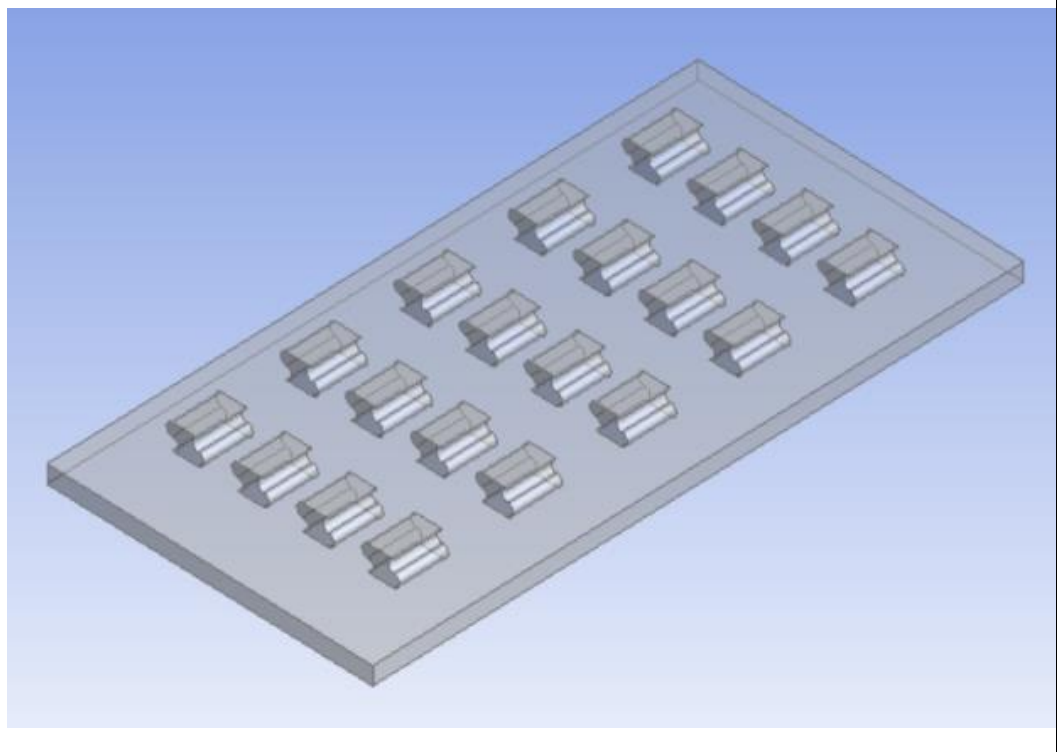
In our simulation we studied three cases including two types of baffles:

	R (radius) cm	L (length) cm	W (width) cm	H (height) cm
Baffle 1	1.25	8	15	5
Baffle 2	1.75	8	15	7

Table III.2: the baffle's dimensions.

- ✓ Case 1 including baffle 1 in a series form;
- ✓ Case 2 including baffle 2 in a series form;
- ✓ Case 3 including baffle 2 in a quincunxes form.

All forms are shown in the table III.3 below:

	Case 1
	Case 2

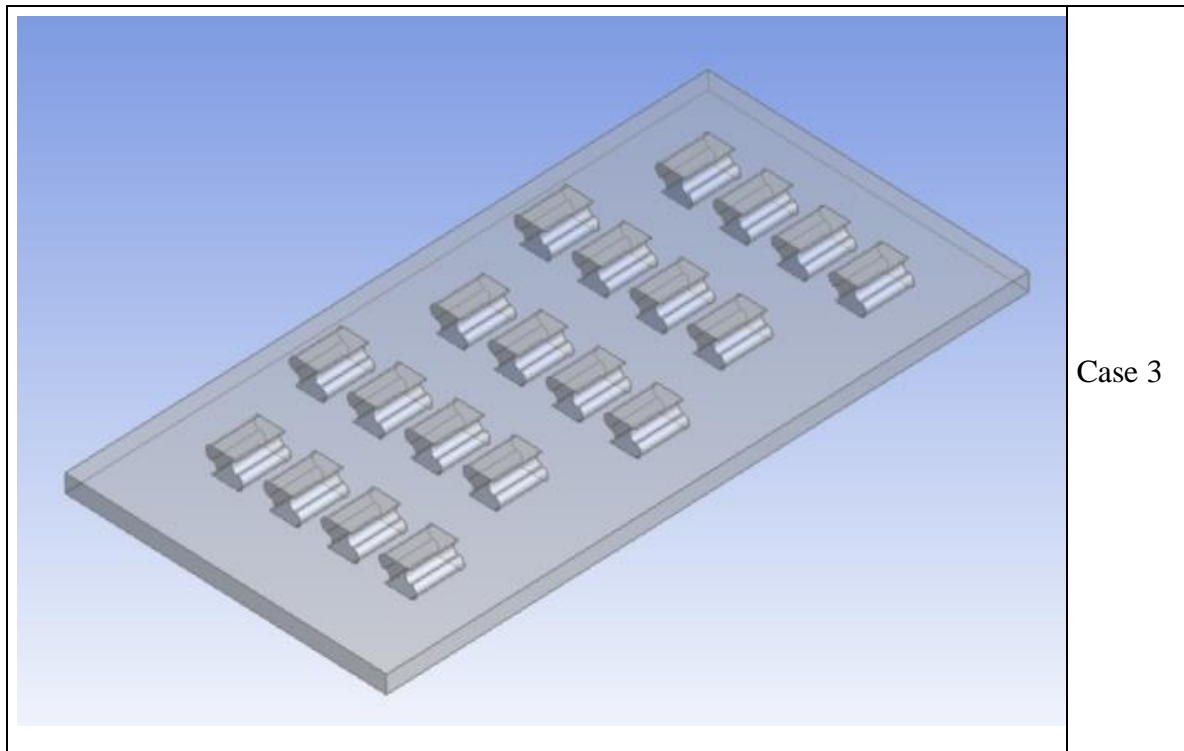


Table III.3: a table that shows the different baffle's positions.

III.7 Mathematical formulation

III.7.1 Simplified assumptions

To be able to solve the equations in this numerical study, we adopted the following simplifying assumptions:

- Stationary flow with laminar mode.
- The fluid is incompressible and Newtonian.
- The fluid & solid thermo-physical properties are constant.
- The speed and temperature at the collector input are constant and uniform.
- The flow is moving in two-dimensional.

III.7.2 Limit Conditions

The boundary conditions are necessary because a the partial derivative equation has a solution when the boundary conditions for each dependent variable are known.

The limit conditions applied in our study are:

- 1) At the collector input
 - All fluid properties are known.
 - Uniform speed and temperature have been applied for all models.
- 2) At the collector output
 - Atmospheric pressure was applied for all models.
- 3) At the lower wall (isolant)
 - The speed range is zero.
 - The adiabatic condition is applied.
- 4) At the higher wall (glass)
 - The speed range is zero.
- 5) At the obstacle (absorber)
 - The speed range is zero.
 - Transmissibility coefficient τ is imposed.
 - Uniform solar flow is required.

III.7.3 Characteristic Settings

a. Reynolds number

Reynolds number is a dimensionless quantity that is used to determine the type of flow pattern as laminar or turbulent while flowing through a pipe. Reynolds number is defined by the ratio of inertial forces to that of viscous forces. Its equation is:

$$Re = \frac{\rho UL}{\mu} \quad \text{(III.16)}$$

b. The friction coefficient

The friction coefficient expression C_f is defined as follows:

$$C_f = \frac{2\tau_w}{\rho \cdot U^2} \quad (\text{III.17})$$

Where w represents the rate of cutting at the wall, ρ the volume mass, U is the average axial speed of the section.

c. Prandtl number

The Prandtl number expresses the relationship between the kinematic viscosity and thermal diffusiveness of a fluid. Its wording is as follows:

$$Pr = \frac{c_p \mu}{\lambda} \quad (\text{III.18})$$

Where:

μ : Dynamic Viscosity;

λ : Thermal conductivity.

d. Nusselt number

This parameter gives us an indication of the proportion of heat transferred by convection compared to that transferred through conduction.

$$Nu = h \frac{L_c}{\lambda} \quad (\text{III.19})$$

Where:

h : heat transfer coefficient by convection;

L_c : Characteristic length;

λ : thermal conductivity of the fluid.

III.8 Conclusion

In this chapter, we focused on problem mathematical modeling resulting in a system of equations. Following a system of equations, profiled by boundary conditions. The digital modeling steps are the building of geometry, the mesh generation, and the implementation of the "Ansys Fluent." Post processor, Convergence control. However, we have detailed the strategy of digital resolution and mathematical formulation. Subsequently, we gave an overview of discretization methods and steps to follow when digitizing by the finite volume method provided by ANSYS FLUENT software.

References :

[1] Guestal M. "Modélisation de la convection naturelle laminaire dans une enceinte avec une paroi chauffé partiellement " Mémoire de magister, Université de MONTOURI,CONSTANTINE, 2010.

[3] Bouaraour et al Etude numérique d'un capteur solaire plan à double passe muni des chicanes The 4th International Seminar on New and Renewable Energies Unité de Recherche Appliquée en Energies Renouvelables,Ghardaïa – Algeria 24 - 25 Octobre 2016.

[3] Mekroussi S. "Simulation du transfert convectif dans une couche limite turbulente en présence d'obstacle décolle de la paroi " Mémoire de magister, Université IbnKhalidounTiaret, (2007).

[4] Fethi Moussa Boudjema and al, "An experimental investigation of the thermal performance of solar collectors utilizing finned aluminum can pipes" university of AIN TEMOUCHENT (2024).

Chapter IV: Interpretation of the results and discussion

IV.1 Introduction

This chapter delves into digital simulations and their application to solar collector design. We used an ANSYS Fluent post processor as a powerful, computational code based on the finite volume method. This sophisticated software allows us to analyze and predict the dynamic and thermal behavior within the collector under the influence of various baffle geometries.

Explored three distinct baffle configurations, each with unique characteristics that influence heat exchange. The first case presents a baffle with a reduced heat exchange surface. Essentially, it offers less area for the incoming sunlight to interact with the collector. The second case introduces a more elongated baffle, significantly increasing the heat exchange surface. Illustrating a wider road for the sunlight to move down, maximizing its interaction with the collector. Finally, the third throws a quincunx arrangement. This unique baffle layout promises to further alter the heat exchange dynamics.

To truly understand the impact of these baffles configurations, we compared them against uniform solar radiation. This baseline provides a reference point for evaluating how the different baffles geometries influence the collector's performance. We analyzed the effects of varying solar radiation levels and the speed of the three-dimensional airflow within the collector. By observing how these factors interact with each baffle design, we aim to gain valuable insights into optimizing solar collector efficiency.

IV.2 Validation

To ensure validation of the model used by the Ansys Fluent calculation code, the experimental data obtained by AbhayLingayat et al [1] are adopted.

The comparison of the variation in the temperature of the air output of the collector (T_{out}) based on the solar flow obtained numerically experimentally by AbhayLingayat et al [1] was performed and shown in Figure IV.1.

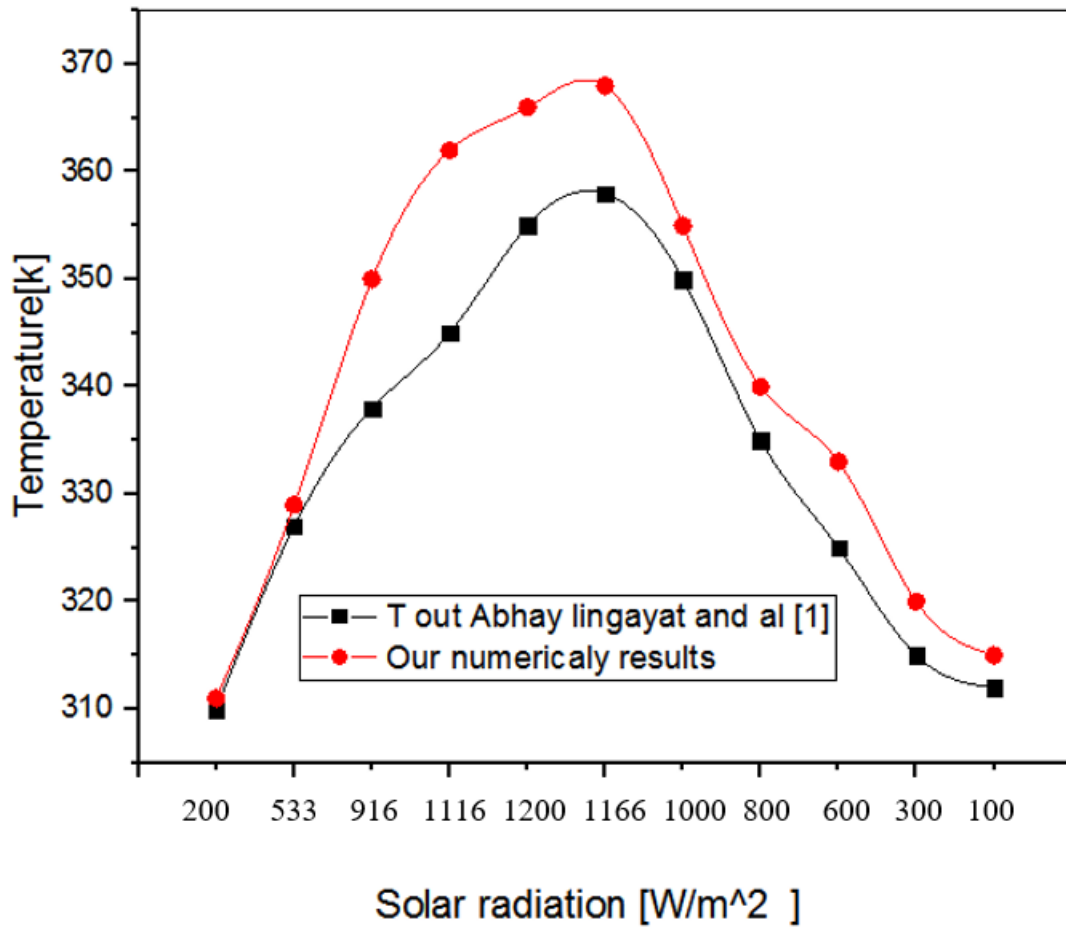


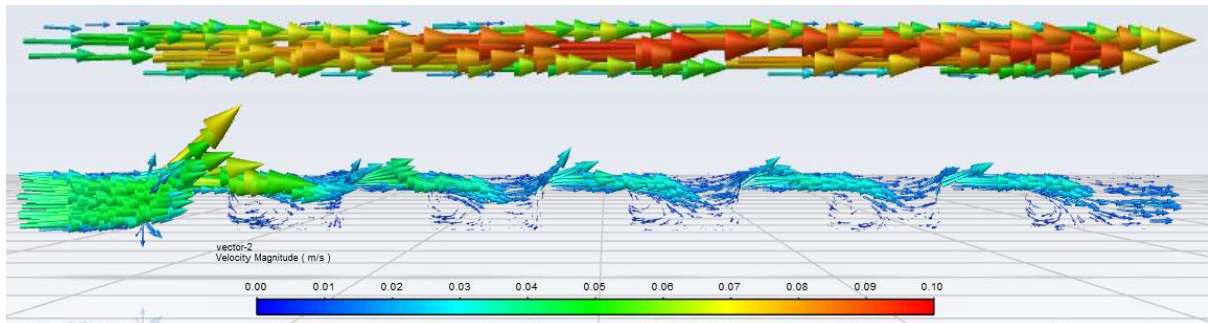
Figure IV.1: air output Temperature of the collector (comparison with the result of AbhayLingayat et al) [1].

IV.3 Results and interpretation

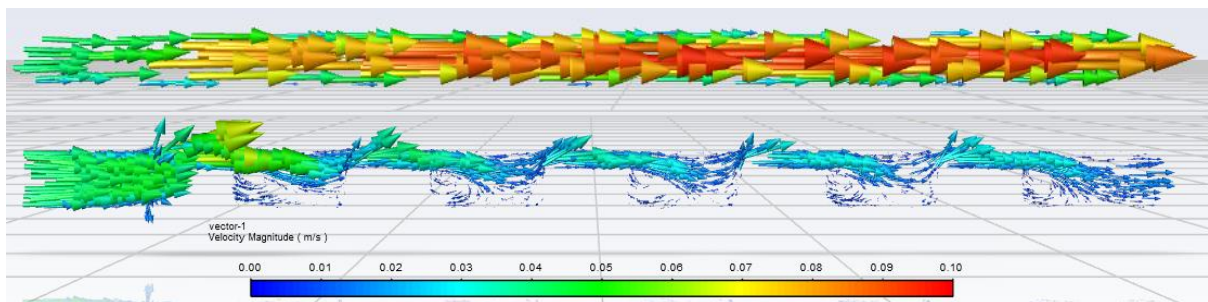
IV.3.1 Dynamic aspect

We applied a velocity of $u=0.04$ m/s and a heat flux of 1200 w/m²

Case 1



Case 2 :



Case 3 :

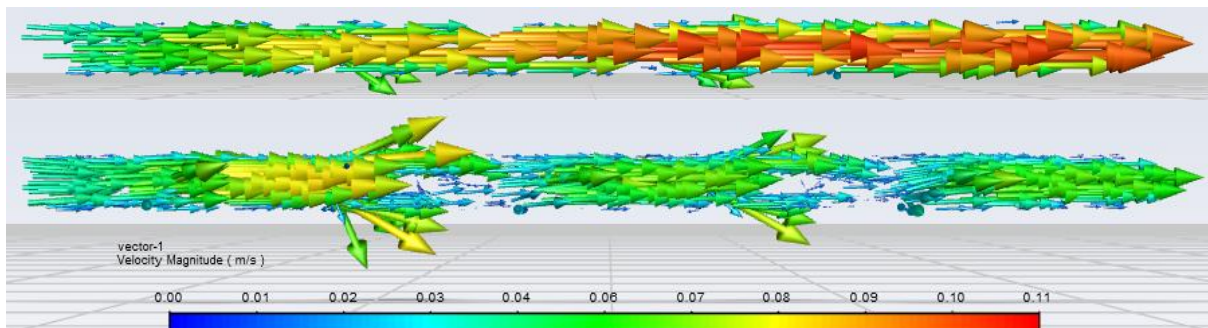


Figure IV.2: Distribution of velocity fields attained from all studied cases.

For case 1 the velocity field within a flat collector with a short baffle (5 cm) placed inside. The short baffle might be intended to slightly disrupt the flow pattern but not significantly alter it.

The 2nd case shows the velocity field when a taller baffle (7 cm) is introduced in a series configuration. This means the baffle is placed directly in line with the flow of the fluid. We were interested in how the taller baffle affects the flow speed and direction compared to the shorter baffle in Case 1.

For the 3rd case, we introduced the same taller baffle (7 cm) but in a "quincunxes" disposition. In a quincunxes arrangement, the baffles are positioned in a specific pattern where each baffle is offset from its neighbors, creating a more staggered layout. We wanted to see how this positioning affects the flow pattern compared to the series configuration (Case 2).

The color scale represents the magnitude of the velocity (speed) at different points within the collector. Since it's a heat transfer application, higher velocities are desirable for better heat exchange.

we can see smoother, straighter velocity fields (arrows) in Case 1 with the short baffle, indicating less disruption to the flow.

Case 2 (long baffle in series) shows more deflection or redirection of the flow due to the taller baffle, potentially creating areas of higher and lower velocities compared to Case 1.

Case 3 (long baffle in quincunxes) displays a more evenly distributed flow compared to Case 2, with the staggered baffle arrangement potentially preventing large-scale flow disruptions.

By comparing the velocity fields (arrow patterns and color distribution) across the cases, we conclude how baffle height and placement influence the flow characteristics within the collector. This information can be crucial for optimizing the collector design for efficient heat transfer.

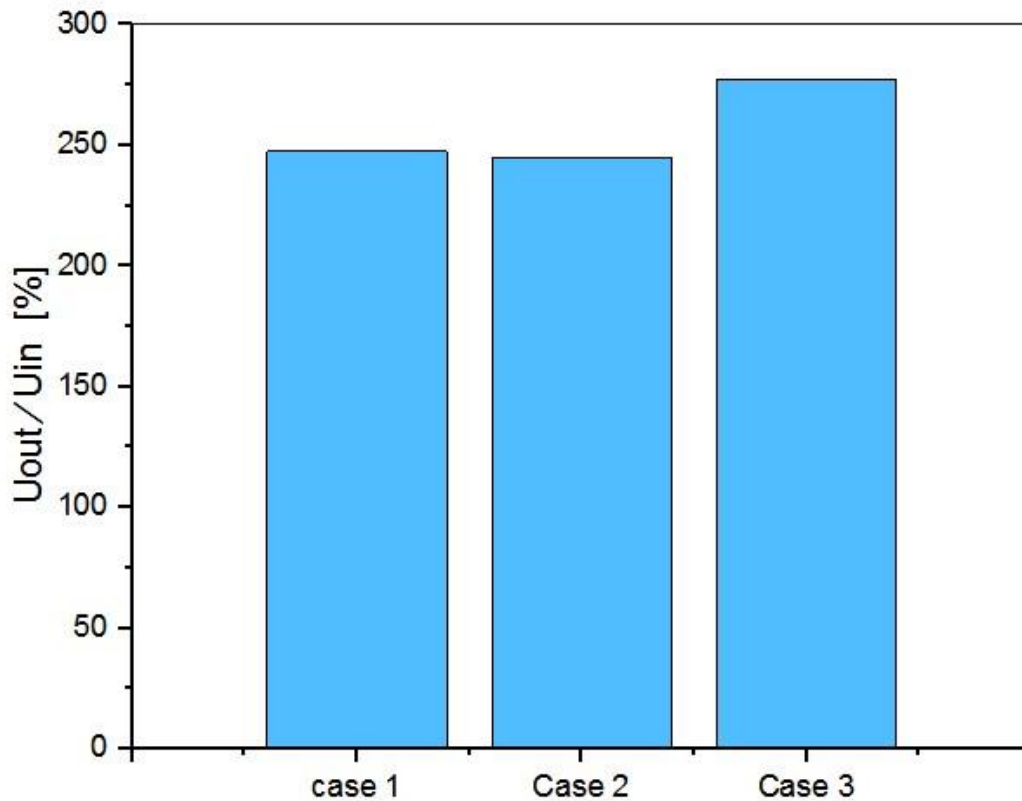


Figure IV.3: variation of the average velocity as a function of the distance of all cases.

The graph in Figure IV.3 contains Case 1, Case 2, and Case 3. Each case therefore refers to a unique set of parameters, including the baffles' use. In Case 1 the graph illustrates the case when the baffles height is 5cm the short baffles. Looking closely at the graph, it may be established that the temperature increases. The change in temperature is smooth, and in this case, this somehow implies that the height factor does not cause a big change in the temperature. Now let us discuss Case 2, the graph represents the same case where long baffles are arranged in series, and each had a height of 7cm; here the graph line increases in temperature to a greater value compared to Case 1.

Finally, in the case 3 the graph represent the scenario with long baffles arranged in quincunxes with a height of 7 cm with temperature standing at a high rate along with the increasing of the heat exchange surface. This establishes that the temperature is highly influenced by the configuration of the baffles in the quincunxes, hence, a faster increase in temperature along with increasing heat exchange surface.

In conclusion, the graph explains how the average temperature varies at different distances from the surfaces with three different configurations of baffle arrangements. Nonetheless, the overall increase in temperature demonstrates the aspect of the relationship between the baffle types and temperature distribution.

IV.3.2 Thermal aspect

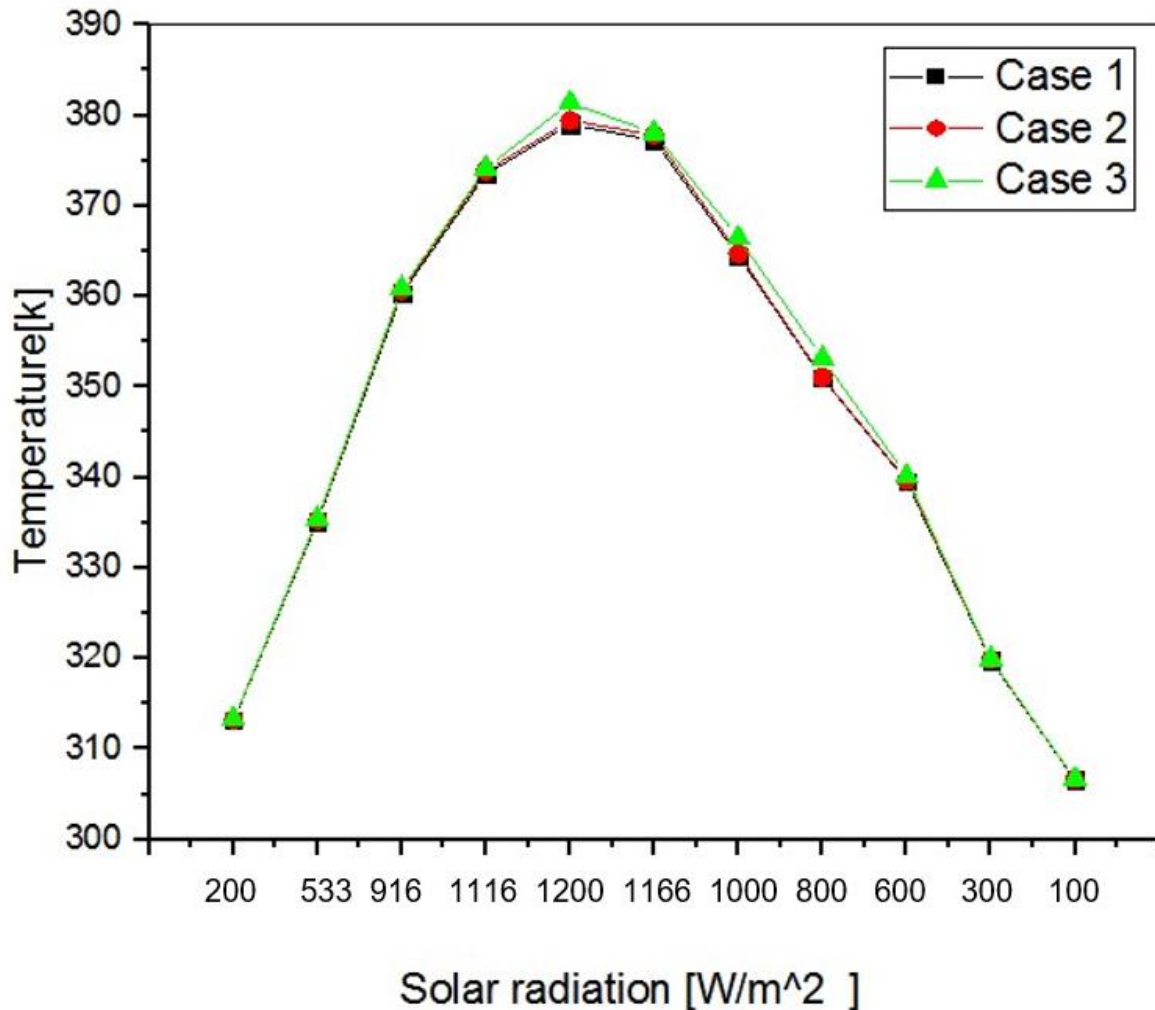


Figure IV.4: Evolution of the temperature at the collector output according to the solar radiation for all studied cases.

The Figure IV.5 shows the correlation between solar radiation (distinct variable) and collector output temperature (impulse variable) implementing the three scenarios.

The horizontal axis charts: “Solar Radiation (W/m²), and the left vertical axis: “Collector Output Temperature (Kelvin).

It is noted however that concerning all the cases above, there is an inverse relationship between the solar radiation and collector temperature, therefore, the solar radiation levels also increase, as well as the collector temperature. Enhanced by the experiment that involves the application of the temperature of solar collector that absorbs solar radiation. As the radiation of the higher temperatures is absorbed by the collector it gets higher. It ultimately reaches a state of balance when it is re-emitting heat energy back into the surrounding environment at the same received rate, from the heat radiation source.

- Case 1 (Short baffle, 5cm): This case shows the hottest collector overall for all radiation levels. This suggests a few possibilities:

The short baffle might not provide the needed speed to direct massive amounts of sunlight towards the absorber plate which means that less heat will be gained due to the short baffle. The fact that short baffle heat exchange surface is the cause of the incapacity of baffles collector to radiate heat back to the surroundings effectively and retain more heat.

- Case 2 (Long baffle in series, 7cm): This case is classified as a mid-range temperature curve. The longer baffles could be:

Better at reflecting sunlight towards the absorber plate resulting in increased heat obtained when compared to Case 1 but could be less efficient than Case 3. Explaining the larger temperature swings are due to the contribution of the collector heat transfer process that is becoming more dynamic.

- Case 3 (Long baffle in quincunxes, 7cm): In this case, the temperature is the highest in the overall configuration. The quincunx arrangement of the long baffles could be:

The position of the angle maximizes the trended path of the sun to reach the absorber plate, promoting the highest heat gain. Improving flows of energy in the collector and effective dissipation of excess energy into the environment reaching the best temperature.

Thus, the solar radiation is inversely related to the collector temperature. The data indicates possible differences in efficiencies among the three types of collectors. Finally, Case 3 (long baffle in quincunxes) seems to be the most efficient design with the highest temperature display of 381.38 K when the radiation reaches a value of 1200 W/m² according to its stable temperature profile and eventually raises the heat gain.

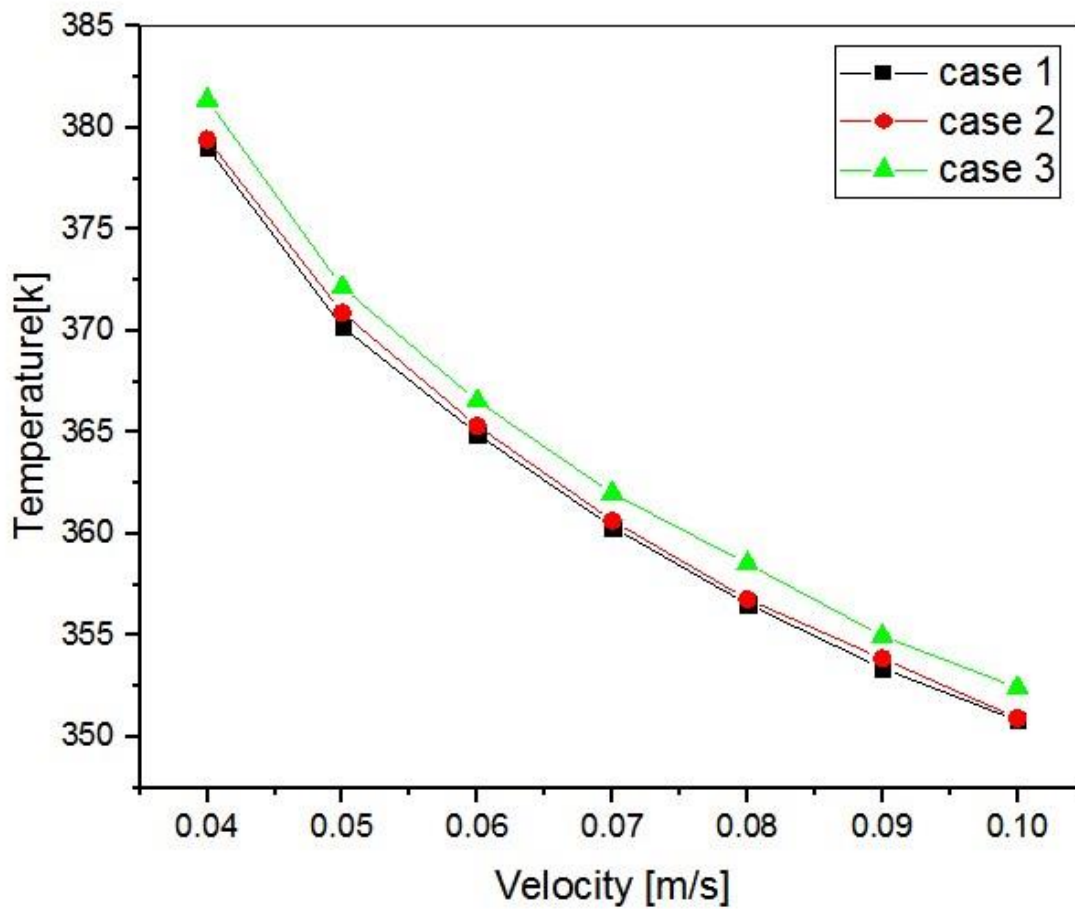


Figure IV.6: Evolution of the temperature at the collector output according to the input velocity for all studied cases.

The Figure IV.7 above reveals that the temperature increases along with increasing velocity for all cases illustrated in the graph. It is the relation between the air velocity at the solar collector inlet (m/s) and the corresponding temperature at the outlet (Kelvin).

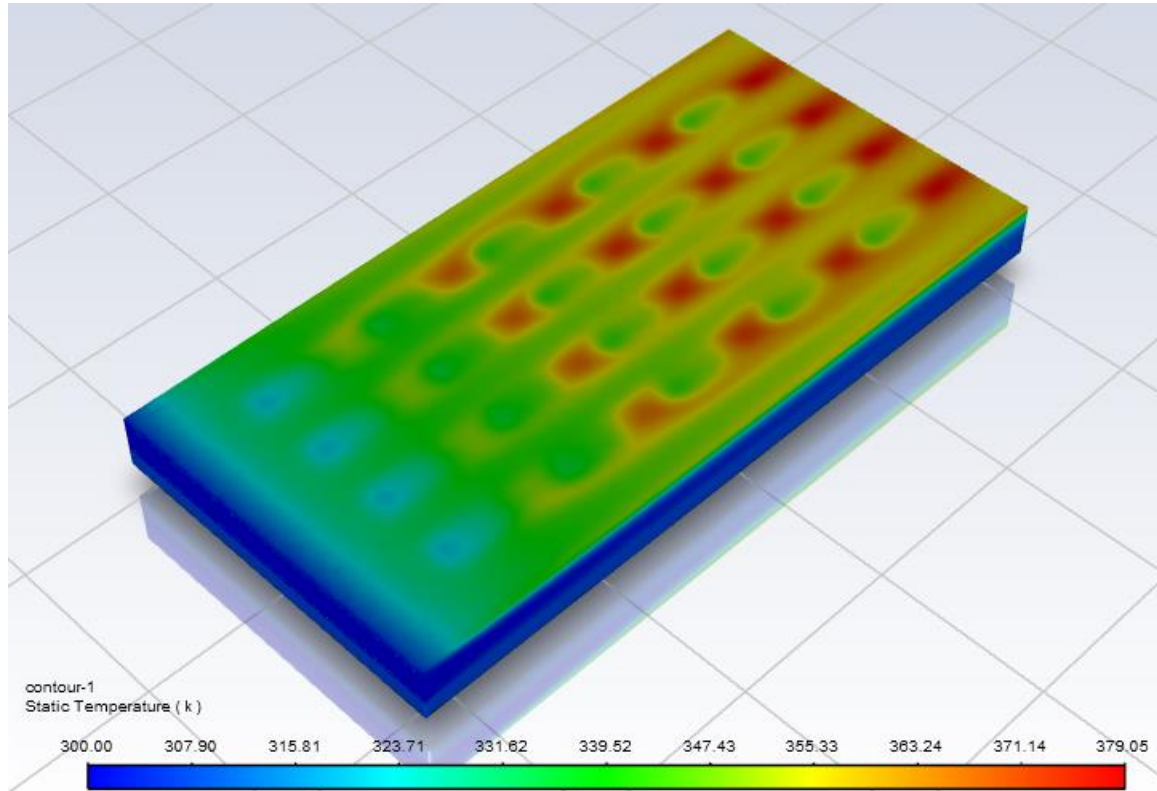
- **Case 1:** This case uses short baffles with a height of 5 cm. Baffles are attached structures in the collectors and can change the fluid flow within the collectors. A short baffle in some cases might produce less resistance compared to other cases.
- **Case 2:** Some curved baffles are particularly used in a series long arrangement with 7 cm high. This configuration might be more cost-effective, but it is likely to increase the fluid pathway to the collector, thus, increasing the duration of the fluid interactions with the collector surface, hence, increasing the heat transfer.
- **Case 3:** This design employs significant baffles (7 cm) into a quincunx formation pattern. Quincunx pattern is like a diagonal grid where elements are shifted from one position from the adjoining rows. It may lead to a better flow distribution of the fluid over the collector, unlikely to use a-series arrangement.

It is also reported that the collector outlet temperature drops with an increase in the pumping speed for all presented cases. It is well established to suspect that reducing fluid velocity more time in dynamic pulsations manner, carry the fluid to spend a long time in the collector, even in a spinning flow shape, which smooths the mixture. Considering that, since we don't provide any accelerating devices to drive the flow by detecting flow dynamic pulsation, this kind of phenomenon may impact with a non-significant trouble-feeding around the air intake orifice, and consequently the same around output orifice, this may explain the gap between the modeling results compared to the experiments study illustrated in the graph of Figure. 4.1, but in general manner, there is a known tolerance to neglect this phenomenon and adopt the assumption in such a model, as the main purpose is to optimize the best baffles/collector design and, hence, promote better heat transfer.

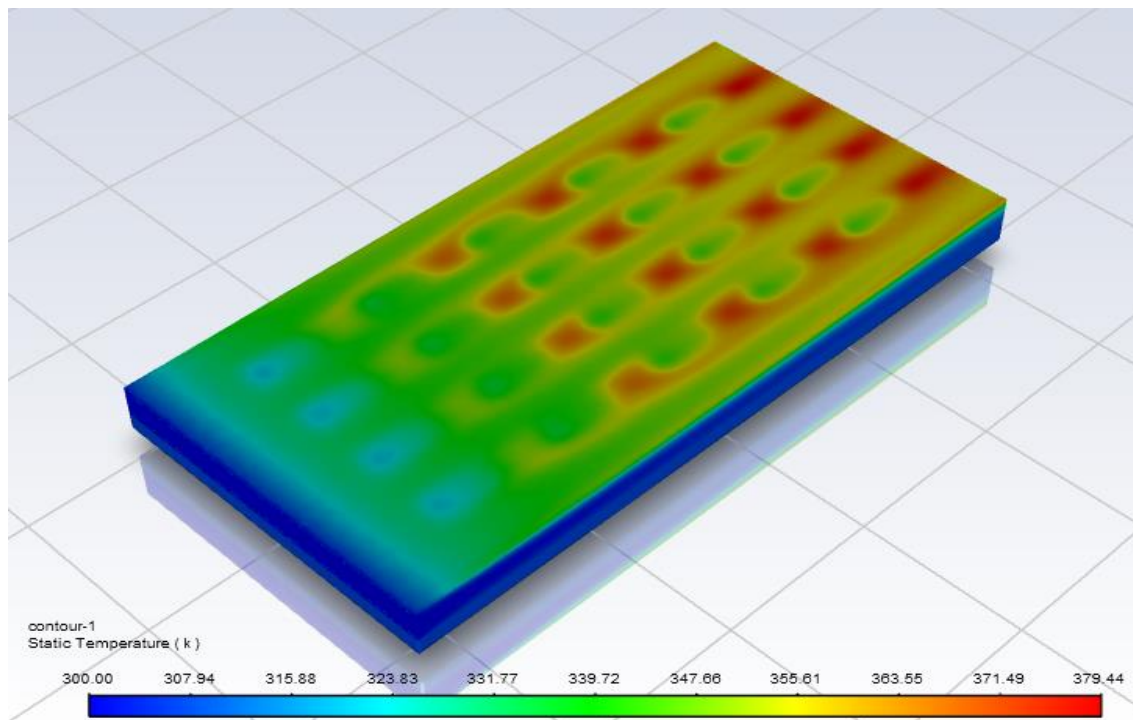
In summary, baffle design has an effect on the thermal performance of a solar collector through the association between flow velocity and outlet temperature.

We applied a velocity of $u=0.04$ m/s and a heat flux of 1200 w/m²

Case 1 :



Case 2 :



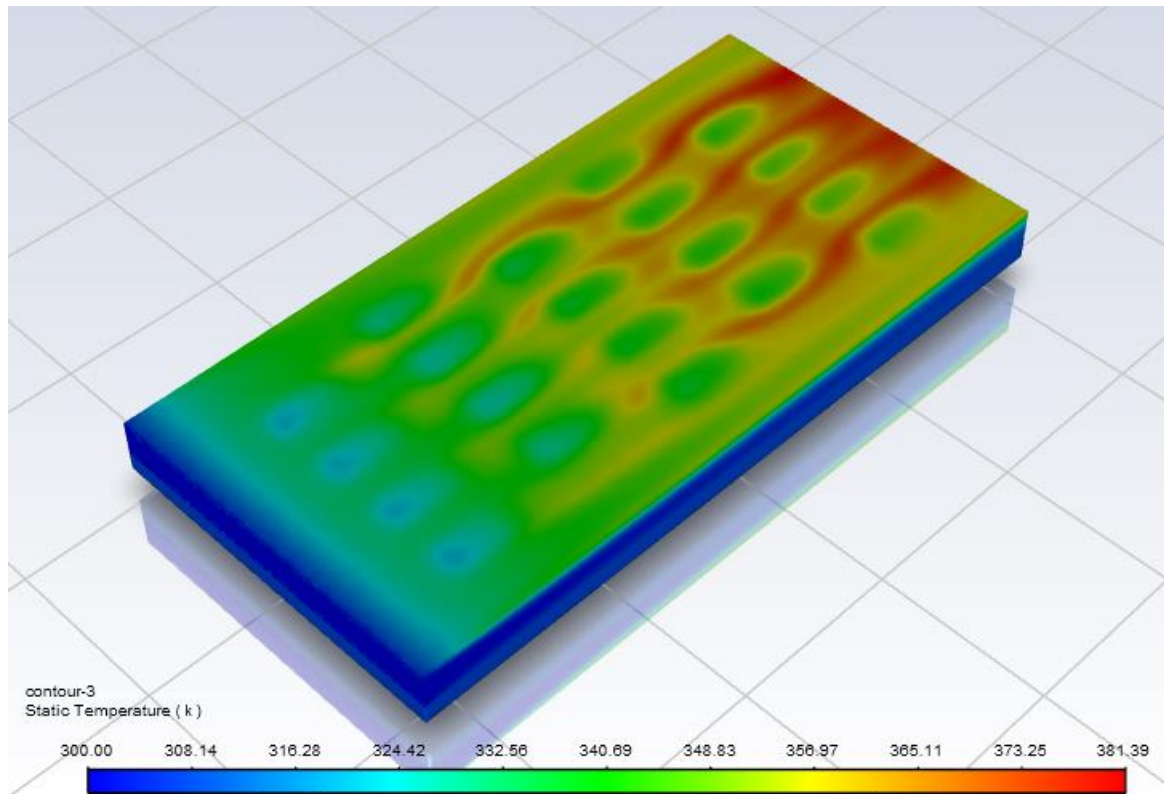
Case 3 :

Figure IV.8: Distribution of temperature fields attained from all studied cases.

The figure IV.6 shows the distribution of temperature in three different cases with a temperature range of 300 Kelvin to 381 Kelvin.

The contour plot in the image shows the temperature distribution across the absorber plate for each of the three cases. The colors in the plot correspond to different temperature ranges. The warmest areas of the absorber plate are shown in red, and the coolest areas are shown in blue.

The 1st and 2nd cases don't have that big of a difference gap resulting in the the airflow section being smaller in the 2nd case

It appears that Case 3, with the long baffle in a quincunx disposition, has a more even temperature distribution than the other two cases. This suggests that Case 3 is the most efficient of the three cases.

IV.4 Conclusion

In this study, we performed a numerical simulation of the thermal and dynamic behavior of the forced convection airflow in different solar collector geometry using Fluent calculation post-processor. The results presented show the temperature and speed contours obtained for different baffle configurations. Compared to the input speed range of [0.04, 0.11] m/s. We highlight the main finding, summarized as follows:

The improvement in heat transfer can be achieved by using a customized wavy-shaped baffle for the absorber.

- The configuration of the higher heat exchange surface presents the highest temperature values, while the cases with a less exchange surface trend the lowest values.
- Regarding the third case, in terms of the flow dynamics, the output speed resulted in a value above the double rate of the input speed.
- The assumption to neglect the flow dynamic pulsations does not impact the main purpose of this study, which consists of optimizing the best configuration (arrangement, shape, and organization) of baffles into the collector. Finding which may serve in other collectors' design studies.

Ending conclusion, in order the best rating of the presented customized configurations, we advance the best efficiency respectively, 3rd case, and 2nd case.

References

- [1] A. Lingayat, V. Chandramohan, V. Raju, Design, development and performance of indirect type solar dryer for banana drying, Energy Procedia, 109 (2017) 409-416.

General conclusion

General Conclusion

The thermal behavior and efficiency of the operating system of a solar collector are influenced by various parameters. However, experimenting with controlling all these parameters is complex and expensive. Therefore, in this study, we undertook an initial approach to solar flow modeling, which allowed us to analyze numerically the thermal and dynamic behavior of a solar collector containing a wavy-shaped absorber. By applying these modeling studies to the context of a flat-glassed solar collector, Our major contribution to this thesis, numerically, is to introduce a new technique and to make a scientific breakthrough aimed at improving the thermal and dynamic performance of a turbulent discharge within a flat-solar collector.

Indeed, we managed to reach a high output temperature for the flat collector, thanks to the whirlwind in the airflow, which also reflects the temperature and flow at the entrance of the drying chamber or the heating.

Digital modeling of solar collectors using ANSYS FLUENT is a crucial tool for avoiding excessive experimental testing costs and improving heat transfer within the airflow.

The incorporation of an obstacle and different geometric shapes is necessary to improve thermal performance and ensure a high output temperature. While studying the solar collector numerically, from a dynamic and thermal point of view, the output velocity of the shrinking model in case 03 was increased by close to 3 times the input velocity.

Finally, we encourage the further studies on the case 03 by adding :

- ✓ A porous environment between the baffles.
- ✓ Add holes to the baffles.
- ✓ Apply other conditions to the limits such as a variable heat flow in time and space.
- ✓ Study the collector for different weather conditions.